

This figure "fig1.gif" is available in "gif" format from:

<http://arxiv.org/ps/astro-ph/9909455v1>

Table 1. Hipparcos and ACT events - lens star properties (astrometry and photometry)

Event #	HIP #	RA				DEC		<i>V</i>	<i>B–V</i>	Other name
		h	m	s	o	'	"			
1	104214	21	6	50.8350	+38	44	29.380	<i>5.20</i>	1.069	61 Cyg A
2	90959	18	33	17.8712	+22	18	55.449	9.016	1.181	V774 Her
3	106122	21	29	46.4600	+45	53	37.083	7.986	0.759	HD 204814
4	57367	11	45	39.2635	–64	50	26.427	11.867	0.196	GJ 440
5	104217	21	6	52.1924	+38	44	3.890	6.208	1.309	61 Cyg B
6	86214	17	37	4.2404	–44	19	0.968	<i>10.94</i>	1.655	GJ 682
7	73734	15	4	19.2795	+60	23	2.956	<i>11.00</i>	1.500	Ross 1051
8	28445	6	0	21.3792	+31	25	50.855	9.505	0.930	HD 250047
9	104214	21	6	50.8350	+38	44	29.380	<i>5.20</i>	1.069	61 Cyg A
10	70890	14	29	47.7474	–62	40	52.867	<i>11.01</i>	1.807	Proxima Cen
11	85523	17	28	39.4569	–46	53	34.986	<i>9.38</i>	1.553	GJ 674
12	64965	13	18	57.0885	–3	4	16.904	<i>10.84</i>	1.009	Ross 484
13	57367	11	45	39.2635	–64	50	26.427	11.867	0.196	GJ 440
14	74234	15	10	13.5770	–16	27	15.521	<i>9.44</i>	0.850	HD 134440
15		18	24	50.7708	+6	56	54.791	11.092	1.224	AC368588
16	87937	17	57	48.9655	+4	40	5.837	<i>9.54</i>	1.570	Barnard Star
17	76074	15	32	13.8455	–41	16	23.108	<i>9.31</i>	1.524	GJ 588
18	33582	6	58	38.3423	–0	28	44.391	9.075	0.579	HD 51754
19	98906	20	5	3.3563	+54	26	11.144	<i>11.98</i>	1.524	V1513 Cyg
20	114622	23	13	14.7435	+57	10	3.498	<i>5.57</i>	1.000	HD 219134
21	61629	12	37	53.1966	–52	0	5.580	10.767	1.470	GJ 479
22	27207	5	46	1.5287	+37	17	9.195	7.417	0.833	HD 38230
23	74926	15	18	39.2706	–18	37	32.607	10.643	1.214	BD–18 4031
24	70890	14	29	47.7474	–62	40	52.867	<i>11.01</i>	1.807	Proxima Cen
25	104217	21	6	52.1924	+38	44	3.890	6.208	1.309	61 Cyg B
26	70890	14	29	47.7474	–62	40	52.867	<i>11.01</i>	1.807	Proxima Cen
27	102923	20	51	6.5386	+7	1	40.380	10.014	0.900	BD+06 4665
28	48336	9	51	8.9608	–12	19	34.728	10.093	1.446	SAO 155530
29	87937	17	57	48.9655	+4	40	5.837	<i>9.54</i>	1.570	Barnard Star
30	105090	21	17	17.7112	–38	51	52.468	<i>6.69</i>	1.397	AX Mic
31	25878	5	31	26.9506	–3	40	19.712	8.144	1.474	HD 36395
32	104214	21	6	50.8350	+38	44	29.380	<i>5.20</i>	1.069	61 Cyg A
33	79537	16	13	49.4874	–57	34	1.492	<i>7.53</i>	0.815	HD 145417
34	87101	17	47	46.1616	–9	36	16.619	9.732	0.672	HD 161770
35	26857	5	42	8.0726	+12	29	35.358	<i>11.56</i>	1.675	V1352 Ori
36	104214	21	6	50.8350	+38	44	29.380	<i>5.20</i>	1.069	61 Cyg A

Rows are ordered by increasing τ (see Table 3). HIP # is the Hipparcos catalog number(blank for entry from ACT only). Right ascension and declination are taken from Hipparcos (or Tycho for ACT-only event) catalog. Equinox J2000, epoch 1991.25. Visual magnitude is in Tycho system if available, or Johnson (italics). Johnson colors are from Hipparcos catalog as well. Multiple entries arise from the fact that a single lens can produce multiple events.

This figure "fig2.gif" is available in "gif" format from:

<http://arxiv.org/ps/astro-ph/9909455v1>

Table 2. Hipparcos and ACT events - lens star properties (distance, kinematic and physical properties)

Event #	μ "/yr ⁻¹	p.a.	v_{rad} km s ⁻¹	M_V	r pc	M M_{\odot}	Class	Sp
1	5.2807	52	-64.28	7.5	3.5	0.5	SD	K5V
2	0.5052	200	37.10	7.2	23.4	0.8	MS	K4V
3	0.5531	50	-83.70	5.6	29.8	0.9	MS	G8V
4	2.6876	97		13.5	4.6	0.6	WD	DC:
5	5.1724	53	-63.48	8.5	3.5	0.4	SD	K7V
6	1.1765	217	-60.00	12.4	5.0	0.2	MS	M5
7	0.6786	285	308.08	9.8	17.6	0.5	MS	M:
8	0.3297	155		6.2	46.1	0.9	MS	K2
9	5.2807	52	-64.28	7.5	3.5	0.5	SD	K5V
10	3.8530	281		15.4	1.3	0.1	MS	M5Ve
11	1.0501	147		11.1	4.5	0.4	MS	K5
12	0.6517	258	126.00	8.1	35.9	0.5	SD	K5
13	2.6876	97		13.5	4.6	0.6	WD	DC:
14	3.6815	196		7.1	29.7	0.6	SD	K0V:
15	0.7359	273		8.4	35.0	0.6	MS	
16	10.3577	356	-106.76	13.2	1.8	0.1	SD	sdM4
17	1.5636	229		10.4	5.9	0.5	MS	M0
18	0.6930	151	-80.59	4.9	68.4	0.8	SD	G0
19	1.4724	232	0.01	11.0	15.8	0.2	SD	M3
20	2.0952	82	-17.79	6.5	6.5	0.8	MS	K3Vvar
21	1.0347	272		10.8	9.7	0.4	MS	M3
22	0.7050	136	-30.90	5.9	20.6	0.9	MS	K0V
23	0.5713	128		8.5	26.2	0.6	MS	
24	3.8530	281		15.4	1.3	0.1	MS	M5Ve
25	5.1724	53	-63.48	8.5	3.5	0.4	SD	K7V
26	3.8530	281		15.4	1.3	0.1	MS	M5Ve
27	0.4333	147		6.6	48.3	0.6	SD	K3
28	1.8487	142	61.01	9.4	13.7	0.4	SD	M0
29	10.3577	356	-106.76	13.2	1.8	0.1	SD	sdM4
30	3.4549	251	23.01	8.7	3.9	0.6	MS	M1/M2V
31	2.2277	160	10.61	9.4	5.7	0.6	MS	M1V
32	5.2807	52	-64.28	7.5	3.5	0.5	SD	K5V
33	1.6491	211	10.01	6.8	13.7	0.6	SD	K0V
34	0.2546	215		4.9	94.3	0.8	SD	G0
35	2.5423	128	103.01	12.7	5.8	0.2	MS	M5
36	5.2807	52	-64.28	7.5	3.5	0.5	SD	K5V

Proper motions are given as intensity and position angle (from Hipparcos, except for ACT-only entry where it is from ACT). Radial velocities are taken from SIMBAD. Absolute magnitude is in the same system as the corresponding visual magnitude. Distances come from Hipparcos trigonometric parallaxes, or from reduced proper motion in the case of ACT-only entry. For mass estimate and class determination see § 3.1 (MS - main sequence star, SD - subdwarf, WD - white dwarf). Spectral class is taken from Hipparcos catalog.

This figure "fig3.gif" is available in "gif" format from:

<http://arxiv.org/ps/astro-ph/9909455v1>

Table 3. Hipparcos and ACT events - source star and event properties

Event #	RA h m s	DEC ° ' "	V	$B-V$	τ hr	d_{2000} "	t_0 yr	β mas	
1	21 6 58.229	+38 45 41.14	10.7		0.1	66.2	2012.5	3064	H
2	18 33 17.603	+22 18 46.65	15.9	0.10	3.1	5.2	2010.2	456	H/A
3	21 29 47.366	+45 53 45.37	16.4	0.96	3.2	7.7	2013.9	366	H/A
4	11 45 48.968	-64 50 33.74	18.1	0.90	3.7	38.8	2014.4	738	H
5	21 6 59.946	+38 45 14.23	18.4	0.61	4.0	69.6	2013.5	636	H
6	17 37 2.520	-44 19 21.96	13.6	0.96	4.9	17.7	2014.9	2022	H
7	15 4 17.808	+60 23 5.38	16.7	0.49	9.1	5.2	2007.7	520	H
8	6 0 21.624	+31 25 44.73	16.9	1.19	9.5	4.0	2012.2	262	H/A
9	21 6 56.938	+38 45 20.65	16.1	0.92	11.0	41.8	2007.9	3686	H
10	14 29 39.583	-62 40 42.81	17.1	1.15	12.1	23.4	2006.1	1360	H
11	17 28 40.850	-46 53 50.64	13.8	1.28	12.6	12.2	2011.2	3401	H
12	13 18 56.199	-3 4 20.84	13.5	0.49	15.7	8.3	2012.6	1136	H
13	11 45 46.125	-64 50 29.29	17.7	0.90	36.5	20.4	2007.5	2805	H
14	15 10 11.993	-16 28 29.09	14.5	0.57	43.3	44.8	2012.2	1862	H
15	18 24 49.870	+6 56 55.68	18.7	0.73	56.0	7.0	2009.5	161	A
16	17 57 47.972	+4 43 0.77	18.4	0.30	58.0	84.9	2008.2	1286	H
17	15 32 11.805	-41 16 47.52	16.4	0.96	60.9	20.0	2012.6	3261	H
18	6 58 38.763	-0 28 53.97	15.7	0.61	66.6	5.4	2007.8	863	H/A
19	20 5 1.087	+54 25 56.10	18.5	0.73	70.1	12.0	2008.2	243	H
20	23 13 18.727	+57 10 12.54	17.0	0.84	74.3	15.7	2007.2	4364	H
21	12 37 50.912	-52 0 5.95	18.4	1.02	78.4	12.1	2011.6	974	H/A
22	5 46 2.356	+37 17 0.80	17.5	0.80	85.3	6.9	2009.6	1349	H/A
23	15 18 40.012	-18 37 39.53	16.9	0.64	112.3	7.6	2013.2	1109	H/A
24	14 29 38.124	-62 40 35.97	17.7	0.74	124.6	34.7	2009.0	3341	H
25	21 6 58.044	+38 44 44.13	16.0	0.41	130.8	34.9	2006.5	9655	H
26	14 29 36.081	-62 40 40.49	17.5	0.80	137.6	47.6	2012.3	3885	H
27	20 51 6.792	+7 1 35.53	18.0	0.57	145.0	2.4	2005.4	464	H/A
28	9 51 10.020	-12 19 57.92	16.6	0.30	181.8	11.8	2006.3	2040	H
29	17 57 47.361	+4 44 5.21	16.5	0.73	184.6	150.0	2014.5	5503	H
30	21 17 13.381	-38 51 59.53	16.0	1.28	187.5	22.3	2005.7	10139	H
31	5 31 27.623	-3 40 56.32	18.7	0.45	197.5	18.6	2008.2	3056	H
32	21 6 58.833	+38 45 32.30	17.3	1.16	202.4	66.8	2012.6	8266	H
33	16 13 47.751	-57 34 27.26	18.6	1.18	215.5	14.9	2009.0	1414	H
34	17 47 46.065	-9 36 19.91	16.7	0.84	256.3	1.5	2005.3	596	H/A
35	5 42 11.049	+12 29 2.60	18.8	0.61	274.1	32.3	2012.7	1170	H
36	21 6 56.066	+38 45 37.57	15.3	0.57	289.7	46.8	2008.3	15873	H

Numeration follows the lens number in tables 1 and 2. Source star's right ascension and declination are at plate epoch, equinox J2000. Visual magnitude is in Tycho, and color in Johnson system (see § 3.1). Event is described by τ (*SIM* observing time), d_{2000} lens-source separation in year 2000.0, t_0 time of closest approach and β , the minimum impact parameter. If $\beta < 300$ mas, τ is calculated using $\beta = 300$ mas (italics). The last column designates whether the event was detected only using the Hipparcos catalog (H), ACT catalog (A), or both (H/A).

This figure "fig4.gif" is available in "gif" format from:

<http://arxiv.org/ps/astro-ph/9909455v1>

Table 4. NLTT events - lens star properties

Event #	Name	RA h m s	DEC ° ' "	Epoch	V	$B-V$	μ "/yr ⁻¹	p.a.	M_V	r pc	M M_{\odot}	Class
1		18 39 28.556	+4 11 48.04	1950.5	15.2	0.84	0.506	240	18.0	2.7	0.6	WD
2		6 21 23.660	+9 38 24.00	1951.9	14.7	0.65	0.390	150	16.5	4.4	0.6	WD
3	255- 27	7 13 4.486	+33 32 34.96	1953.9	17.1	1.04	0.365	168	19.5	3.4	0.6	WD
4	W 843	18 17 50.041	+23 17 55.07	1954.4	14.3	0.73	0.457	265	17.1	2.8	0.6	WD
5	R 619	8 11 54.022	+8 50 31.40	1951.2	12.7	0.92	5.211	167	18.6	0.7	0.6	WD
6	388- 57*	17 36 11.386	+23 48 32.56	1951.5	19.0	0.80	0.184	196	17.7	18.4	0.6	WD
7	755- 18	20 27 30.373	-13 17 36.28	1953.8	17.8	0.42	0.375	215	14.7	40.2	0.6	WD
8	516- 6	20 48 10.249	+12 4 17.36	1952.6	16.9	0.88	0.222	139	18.3	5.3	0.6	WD
9	838- 25	6 14 16.134	-23 10 16.91	1982.6	14.8	0.74	0.388	156	17.2	4.4	0.6	WD
10	385- 32	16 6 36.064	+24 28 56.72	1950.4	18.0	0.96	0.316	191	18.9	6.7	0.6	WD
11	105-469	19 57 12.362	+57 52 17.37	1952.6	14.1	0.57	0.355	223	15.9	4.4	0.6	WD
12	543- 33	7 50 14.731	+7 12 55.88	1956.0	16.2	0.65	1.778	173	16.5	8.8	0.6	WD
13	R 627	11 24 16.300	+21 21 36.47	1955.2	13.9	0.49	1.050	270	15.3	5.1	0.6	WD
14	634- 1	19 56 30.642	-1 1 58.60	1951.6	13.1	0.30	0.790	211	13.9	7.1	0.6	WD
15	302- 31	4 30 51.262	+28 12 30.64	1955.8	17.6	0.92	1.038	143	18.6	6.3	0.6	WD
16		1 16 23.653	+24 19 57.57	1954.7	15.0	1.16	1.841	112	20.3	0.9	0.6	WD
17		0 35 49.472	+52 41 20.44	1954.8	12.0	1.20	0.789	102	10.0	25.2	0.3	SD
18	806- 18	17 0 41.920	-18 44 6.77	1954.4	15.9	0.92	0.417	190	18.6	2.9	0.6	WD
19	329- 21	16 1 47.563	+30 30 56.39	1950.4	18.7	0.80	0.217	151	17.7	16.1	0.6	WD
20	515- 3	20 19 4.748	+12 36 2.93	1951.6	14.7	1.04	1.213	185	19.5	1.1	0.6	WD
21	197- 4	2 25 40.397	+42 27 9.22	1952.0	18.0	0.73	0.232	103	17.1	15.3	0.6	WD
22	650-237	2 31 56.521	-8 31 49.97	1953.9	15.7	1.04	0.302	164	8.7	248.5	0.4	SD
23	W 1084	20 43 14.497	+55 19 31.91	1952.7	14.7	1.08	1.915	28	19.7	1.0	0.6	WD
24		17 46 38.204	-12 58 1.65	1954.5	13.8	0.80	0.687	239	17.7	1.7	0.6	WD
25	722- 1	7 13 39.010	-13 27 8.92	1958.9	14.3	0.80	1.277	153	17.7	2.1	0.6	WD
26		5 10 28.686	+31 17 40.40	1955.8	16.6	0.80	0.690	104	17.7	6.1	0.6	WD
27	106- 38	20 14 42.346	+61 46 2.35	1952.7	16.5	0.96	0.698	26	18.9	3.4	0.6	WD
28	816- 34	21 0 36.543	-18 16 49.97	1982.5	16.8	0.45	0.198	207	15.2	20.6	0.6	WD
29	752- 15	19 9 56.654	-13 30 18.48	1951.7	14.5	0.45	0.345	202	15.0	7.8	0.6	WD
30		23 18 6.829	+49 28 28.65	1954.6	12.8	0.77	0.320	177	6.5	177.2	0.6	SD
31	503- 16	15 35 22.414	+13 6 40.07	1950.4	17.6	1.04	0.283	301	19.5	4.2	0.6	WD
32	707- 8	1 9 2.850	-10 42 12.40	1951.9	16.0	0.26	0.198	98	13.6	30.5	0.6	WD

Table 4—Continued

Event #	Name	RA				DEC		Epoch	V	$B-V$	μ "/yr ⁻¹	p.a.	M_V	r pc	M M_\odot	Class
		h	m	s	o	'	"									
33	St 2051B*	4	31	1.299	+59	0	32.25	1953.1	13.1	0.77	2.383	144	17.4	1.4	0.6	WD
34		5	50	22.924	+17	19	40.48	1951.9	15.4	0.38	0.589	143	14.4	15.6	0.6	WD
35	911- 9	13	24	27.296	-33	16	12.63	1985.3	14.6	0.83	0.678	151	17.9	2.6	0.6	WD
36	751- 1	19	3	17.335	-13	33	51.29	1951.6	16.1	1.04	0.780	226	19.5	2.1	0.6	WD
37	780- 20	6	37	21.434	-18	58	55.24	1982.9	17.6	0.69	0.188	134	16.9	13.7	0.6	WD
38		13	38	26.916	-2	52	3.11	1952.1	15.0	0.96	3.713	290	18.9	1.7	0.6	WD
39	90-134	9	17	45.873	+58	26	14.34	1954.9	14.8	1.04	1.134	180	19.5	1.2	0.6	WD
40	29- 23	0	43	57.017	+75	12	26.58	1954.7	17.8	0.53	0.302	104	15.6	27.2	0.6	WD
41	W 1106	21	8	1.888	+59	44	46.38	1952.6	13.5	1.00	2.098	209	19.2	0.8	0.6	WD
42	728- 31	9	50	42.938	-12	16	17.45	1956.0	17.2	1.00	0.340	173	19.2	4.1	0.6	WD
43	664- 28	8	14	36.469	-8	1	12.87	1953.2	17.6	1.08	0.319	180	19.7	3.8	0.6	WD
44		23	6	20.168	+65	3	40.06	1952.6	15.1	1.31	0.328	127	10.9	69.5	0.2	SD
45	294- 61	1	10	45.192	+27	58	23.76	1952.7	15.8	0.61	0.235	235	16.2	8.2	0.6	WD
46		19	38	48.799	+35	11	59.25	1952.5	14.6	1.00	0.786	359	8.4	177.3	0.4	SD
47	452- 1	19	21	41.880	+20	53	11.01	1953.6	13.4	1.35	1.751	213	11.2	26.8	0.2	SD
48	921- 25	18	6	31.134	-30	9	46.02	1977.5	15.8	0.26	0.252	158	13.5	49.0	0.6	WD
49	203- 15	5	28	24.141	+39	45	8.73	1953.0	15.0	0.49	0.230	160	15.3	8.4	0.6	WD
50		22	36	37.952	+53	3	16.60	1953.8	16.7	-0.01	0.260	226	11.5	107.9	0.6	WD
51	48-813	23	5	14.278	+71	23	4.06	1952.6	18.9	0.38	0.277	56	14.4	78.4	0.6	WD
52	264- 49	11	24	9.492	+35	47	30.87	1953.2	18.2	1.04	0.277	269	19.5	5.6	0.6	WD
53	399-299	22	1	5.918	+29	9	37.25	1951.7	15.7	0.53	0.598	94	15.6	10.4	0.6	WD
54	689- 11	17	55	49.491	-7	35	52.55	1954.5	12.0	0.88	0.253	234	7.5	81.0	0.5	SD
55	666- 14	8	55	22.441	-4	3	19.07	1950.0	19.4	1.20	0.414	128	20.6	5.6	0.6	WD
56	101- 15*	16	34	26.515	+57	8	51.68	1955.3	12.8	1.08	1.620	316	9.0	57.8	0.4	SD
57	W 1084	20	43	14.497	+55	19	31.91	1952.7	14.7	1.08	1.915	28	19.7	1.0	0.6	WD
58	404- 7	23	57	50.183	+19	48	54.17	1954.7	16.6	0.69	0.308	33	16.8	9.0	0.6	WD
59	16- 36	5	37	59.136	+79	31	7.02	1955.0	18.4	0.65	1.192	143	16.5	24.3	0.6	WD
60	569- 98	18	2	32.463	+5	45	2.88	1950.5	18.4	0.49	0.472	205	15.3	40.3	0.6	WD
61		21	35	19.125	+46	33	41.32	1952.7	16.8	0.61	0.459	200	16.2	13.0	0.6	WD
62	187- 7*	21	35	19.125	+46	33	41.32	1952.7	16.8	0.61	0.459	200	16.2	13.0	0.6	WD
63		3	43	49.491	+63	40	30.51	1954.1	12.6	0.92	0.962	142	7.8	90.2	0.5	SD
64	627- 16	17	15	24.815	+1	19	17.36	1954.6	15.2	1.08	0.369	287	9.0	174.6	0.4	SD

Table 4—Continued

Event #	Name	RA h m s	DEC ° ' "	Epoch	V	$B-V$	μ "/yr ⁻¹	p.a.	M_V	r pc	M M_\odot	Class
65		4 48 8.474	+48 32 33.92	1953.8	16.1	0.88	0.503	123	18.3	3.7	0.6	WD
66	275- 67	16 35 14.669	+35 47 26.61	1954.5	13.6	1.35	0.221	236	9.2	75.2	0.6	MS
67	358-663	4 18 24.239	+22 11 51.20	1950.9	17.7	1.04	0.404	136	19.5	4.4	0.6	WD
68	897- 14	7 38 26.674	-27 27 55.79	1981.1	14.7	0.61	0.294	120	16.2	7.1	0.6	WD
69	795- 43	12 38 42.283	-19 21 39.49	1954.2	12.8	1.04	0.356	301	8.7	65.4	0.4	SD
70		20 34 2.949	+64 19 16.42	1952.6	13.1	0.96	0.436	254	8.1	100.4	0.5	SD
71	229- 15	18 32 54.614	+42 25 49.90	1955.6	18.3	1.00	0.199	195	19.2	6.9	0.6	WD
72	+53:2911*	22 32 49.389	+53 47 35.90	1952.7	10.0	1.16	1.318	86	9.6	11.9	0.3	SD
73	Pl 1	16 8 16.115	-10 25 14.55	1954.3	14.4	1.00	1.354	195	19.2	1.1	0.6	WD
74	*	1 47 57.166	+60 7 37.36	1954.8	13.0	1.08	0.238	228	9.0	63.4	0.4	SD
75	+15:4074B*	20 11 14.684	+16 10 48.99	1951.7	13.4	0.96	0.572	313	8.1	115.3	0.5	SD
76		2 7 2.738	+49 39 3.27	1953.9	12.6	0.77	0.498	150	6.5	161.6	0.6	SD
77	R 201	21 40 27.505	+54 0 27.19	1955.9	14.5	1.08	0.414	76	9.0	126.5	0.4	SD
78	R 28	4 13 0.374	+52 37 18.90	1954.8	13.4	1.12	0.910	203	9.3	64.4	0.4	SD
79	W 1471	17 42 13.351	-8 48 38.49	1954.5	13.2	1.12	0.965	240	9.3	58.7	0.4	SD
80	206- 11	7 11 9.969	+43 30 24.23	1954.2	15.4	1.08	0.680	146	9.0	191.4	0.4	SD
81		1 48 47.971	+55 2 7.77	1954.8	14.0	0.84	0.280	96	7.2	230.0	0.5	SD
82	693- 14	19 38 31.489	-2 51 12.08	1953.8	11.1	0.80	0.286	111	6.8	71.6	0.6	SD
83	497- 4	13 8 26.655	+12 26 37.11	1955.4	13.9	1.16	0.288	268	9.6	71.7	0.3	SD
84	L 560-9	18 8 7.463	-30 55 37.13	1977.5	16.4	0.70	0.300	204	16.9	10.4	0.6	WD
85	129- 60	11 16 37.394	+53 5 17.78	1950.2	15.1	0.69	0.300	218	16.8	4.5	0.6	WD
86	377- 12	12 33 50.545	+22 34 32.05	1955.4	18.2	1.08	0.307	260	19.7	5.0	0.6	WD
87	722- 1	7 13 39.010	-13 27 8.92	1958.9	14.3	0.80	1.277	153	17.7	2.1	0.6	WD
88		3 48 26.217	+51 14 27.43	1954.8	12.7	0.49	0.498	131	15.3	2.9	0.6	WD
89	152- 10	1 38 30.185	+47 32 24.64	1953.8	17.9	0.84	0.362	107	18.0	9.5	0.6	WD
90	74- 42	21 7 36.722	+66 20 49.15	1952.6	17.3	0.73	0.184	88	17.1	11.1	0.6	WD
91		5 44 0.906	+40 57 36.74	1953.0	15.3	0.18	1.229	147	13.0	29.1	0.6	WD
92	447- 63	17 7 15.732	+19 25 51.93	1954.5	13.0	1.12	0.180	166	7.7	113.5	0.7	MS
93	555- 5	12 21 49.938	+6 44 7.76	1956.2	14.2	1.04	0.732	174	8.7	124.5	0.4	SD
94	747- 11	17 11 25.904	-14 47 40.79	1954.5	14.0	0.18	0.371	132	13.0	16.0	0.6	WD
95	575- 26	20 34 31.829	+7 57 32.56	1951.6	14.7	1.20	0.374	82	10.0	87.5	0.3	SD
96	753- 2	19 34 52.751	-12 20 53.98	1951.6	16.9	0.92	0.456	218	18.6	4.5	0.6	WD

Table 4—Continued

Event #	Name	RA				DEC		Epoch	V	$B-V$	μ "/yr ⁻¹	p.a.	M_V	r pc	M M_\odot	Class
		h	m	s	o	'	"									
97	642- 53*	23	21	16.021	+1	2	36.61	1953.8	18.6	0.53	0.267	207	15.6	39.4	0.6	WD
98	642- 52	23	21	16.021	+1	2	36.61	1953.8	18.6	0.53	0.267	207	15.6	39.4	0.6	WD
99	155- 61	3	21	26.521	+46	57	47.07	1954.8	17.7	1.00	0.277	143	19.2	5.2	0.6	WD
100	697- 45	21	31	21.313	-5	11	16.37	1954.5	14.7	1.04	0.374	96	8.7	156.8	0.4	SD
101	787- 49	9	29	42.151	-17	32	36.06	1954.3	15.4	0.22	0.447	134	13.3	27.2	0.6	WD
102		5	44	0.906	+40	57	36.74	1953.0	15.3	0.18	1.229	147	13.0	29.1	0.6	WD
103	372- 4	10	20	42.743	+20	27	58.49	1955.3	18.5	0.45	0.265	202	15.0	49.5	0.6	WD
104	209- 18	8	33	15.955	+40	56	14.51	1953.2	17.7	1.00	0.229	173	19.2	5.2	0.6	WD
105	R 19	2	19	0.361	+35	21	39.44	1951.8	12.4	1.12	0.792	122	9.3	40.6	0.4	SD
106	753- 7	19	36	8.090	-11	40	39.10	1951.6	17.5	0.88	0.248	186	18.3	7.0	0.6	WD
107		12	38	33.755	+35	13	19.72	1950.4	14.6	1.04	0.267	223	8.7	149.7	0.4	SD
108	*	21	10	59.853	+46	57	47.07	1952.6	14.2	0.84	0.395	218	7.2	252.2	0.5	SD
109	544- 37	8	15	18.921	+4	55	46.71	1949.9	17.7	1.00	0.214	162	8.4	738.9	0.4	SD
110	*	13	14	9.168	+6	18	43.68	1956.2	15.5	0.92	0.334	216	7.8	342.9	0.5	SD
111	572- 1	19	22	4.532	+7	2	51.55	1950.6	12.2	1.23	0.836	242	10.3	24.5	0.3	SD
112	336- 6*	19	7	38.151	+32	31	45.33	1950.5	11.8	0.96	1.635	49	8.1	55.2	0.5	SD
113	29- 23	0	43	57.017	+75	12	26.58	1954.7	17.8	0.53	0.302	104	15.6	27.2	0.6	WD
114		23	57	40.446	+23	19	8.48	1950.6	11.9	0.96	1.460	135	8.1	57.8	0.5	SD
115	R 341	3	6	15.472	+51	3	45.93	1953.8	12.9	1.00	0.846	124	8.4	81.0	0.4	SD
116	44- 47	17	37	24.418	+71	4	16.15	1953.7	12.2	1.04	0.482	143	8.7	49.6	0.4	SD
117	813- 32	19	57	26.933	-17	30	16.64	1953.6	14.5	1.04	0.499	98	8.7	143.0	0.4	SD
118		18	47	15.688	-17	25	57.59	1954.5	14.1	0.88	0.480	201	7.5	213.1	0.5	SD
119		5	48	23.867	+7	45	50.87	1955.9	14.2	1.04	0.276	165	8.7	124.5	0.4	SD
120	751- 12	18	55	11.684	-9	3	45.85	1951.6	12.8	0.84	0.332	321	7.2	132.4	0.5	SD
121	R 66	5	49	56.578	+36	50	46.56	1954.9	12.2	1.12	0.510	165	9.3	37.0	0.4	SD
122	152- 27	15	29	29.623	-61	46	28.80	1980.3	15.9	0.45	0.210	189	15.0	23.2	0.6	WD
123	297- 12	2	11	57.902	+32	21	57.01	1954.8	15.6	1.27	0.567	114	10.6	99.0	0.3	SD
124	192- 23	0	1	45.551	+41	36	2.66	1954.8	14.5	1.04	0.299	141	8.7	143.0	0.4	SD
125	877- 22	22	52	25.887	-22	20	1.71	1982.8	13.2	1.15	0.291	192	9.6	52.7	0.3	SD
126	391- 2*	18	41	8.443	+24	46	59.89	1951.5	15.7	0.61	0.501	85	16.2	7.9	0.6	WD
127	48-526	22	8	58.982	+70	41	40.98	1952.6	18.2	0.69	0.247	44	16.8	18.9	0.6	WD
128	60-136	8	52	31.833	+68	0	24.39	1954.9	18.3	0.96	0.180	218	18.9	7.7	0.6	WD

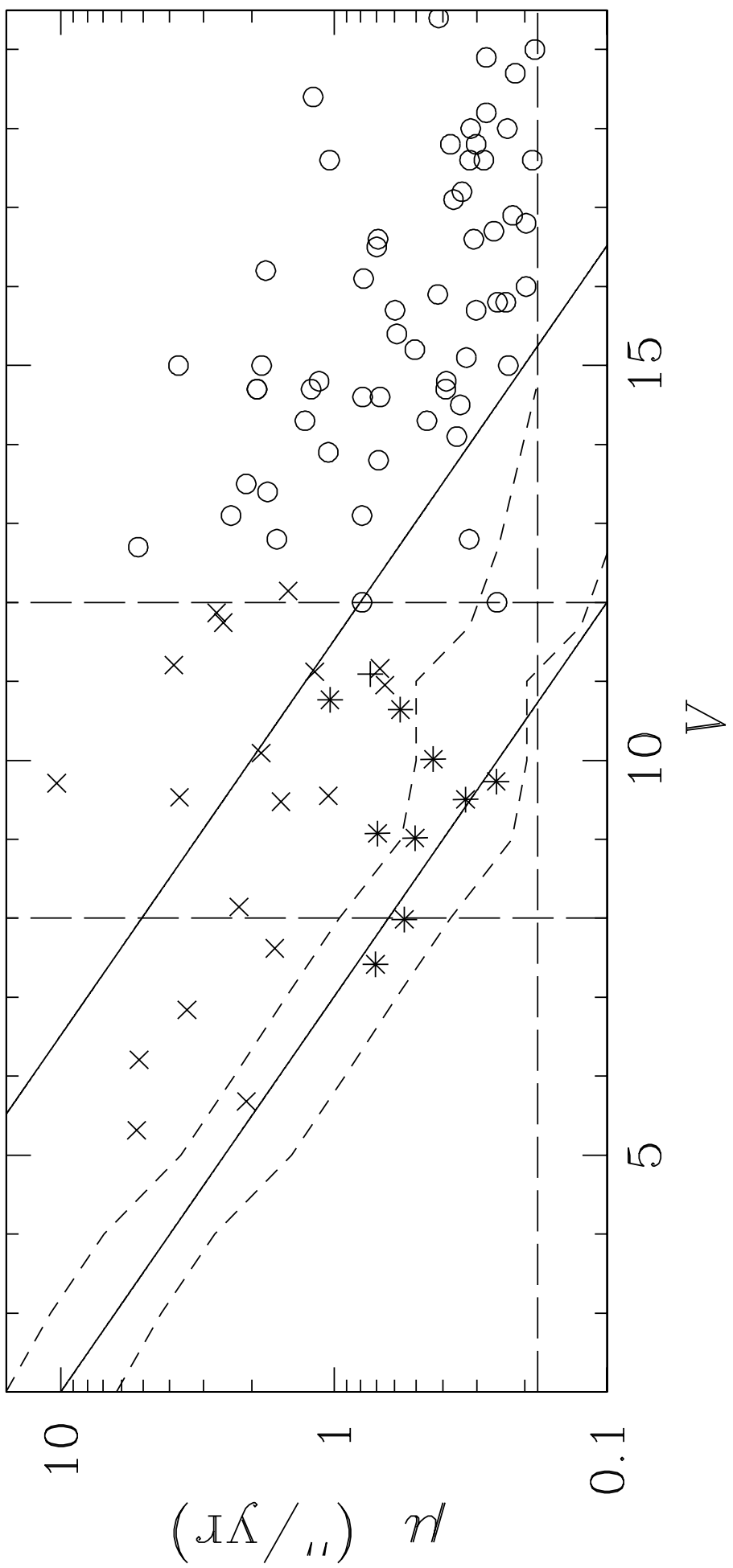
Table 4—Continued

Event #	Name	RA h m s	o	DEC ' "	Epoch	V	$B-V$	μ "/yr ⁻¹	p.a.	M_V	r pc	M M_\odot	Class	
129	700- 35	22 32	47.802	-5	57 10.12	1954.5	11.4	0.73	0.266	242	6.2	110.1	0.6	SD
130	92- 78	10 17	11.561	+60	11 54.99	1954.0	18.8	1.00	0.293	210	19.2	8.6	0.6	WD
131		14 55	2.827	+43	1 45.58	1955.2	11.5	0.77	0.302	207	6.5	97.4	0.6	SD
132		15 27	44.992	-9	1 18.36	1955.4	15.1	1.16	0.318	172	9.6	124.6	0.3	SD
133	82- 44	3 0	58.173	+59	36 40.78	1954.1	14.8	1.08	0.223	92	9.0	145.2	0.4	SD
134	241- 23	0 31	3.915	+36	40 50.36	1951.8	15.4	1.00	0.257	174	8.4	256.2	0.4	SD
135	809- 20	18 15	13.218	-19	23 41.55	1954.5	12.4	0.61	0.382	162	5.3	264.0	0.7	SD
136		23 10	3.417	+63	58 15.30	1952.6	14.1	0.22	0.400	175	13.3	14.9	0.6	WD
137		23 9	36.226	+33	12 40.09	1954.7	12.7	1.00	0.366	75	8.4	73.9	0.4	SD
138	678- 54	13 42	12.160	-5	59 1.36	1952.4	18.6	0.69	0.235	234	16.8	22.7	0.6	WD
139		23 15	24.163	+9	44 42.72	1951.6	13.3	0.80	0.412	74	6.8	197.3	0.6	SD
140	763- 7*	23 42	19.222	-13	56 29.83	1953.6	15.1	0.92	0.295	57	7.8	285.2	0.5	SD
141		21 52	10.747	+27	25 36.71	1951.5	13.9	0.92	0.806	159	7.8	164.1	0.5	SD
142	R 28	4 13	0.374	+52	37 18.90	1954.8	13.4	1.12	0.910	203	9.3	64.4	0.4	SD
143	458- 12	21 36	9.978	+19	5 7.40	1951.7	11.5	0.69	0.326	76	5.9	130.3	0.7	SD
144	552- 14	11 11	55.687	+3	37 32.09	1955.3	17.8	0.42	0.377	255	14.7	40.2	0.6	WD
145	- 3:5711*	23 49	22.223	-2	34 26.83	1954.6	10.8	0.65	0.260	93	5.6	111.8	0.7	SD
146	R 600	4 41	20.419	+22	54 52.55	1950.9	12.6	0.88	0.650	145	7.5	106.8	0.5	SD
147		17 30	20.956	+19	12 37.12	1951.5	13.1	1.00	0.396	104	8.4	88.8	0.4	SD
148	901- 11	9 6	40.366	-30	12 19.16	1979.7	15.7	0.51	0.193	156	15.5	16.7	0.6	WD
149	T 9	17 18	46.497	-29	46 5.88	1981.4	12.9	1.31	0.242	109	8.9	55.2	0.6	MS
150		9 43	46.790	-7	3 28.41	1953.0	16.1	0.42	0.441	188	14.7	18.4	0.6	WD
151		15 24	38.145	-6	49 7.71	1955.4	15.5	1.16	0.477	212	9.6	149.8	0.3	SD
152		0 28	51.956	+50	22 27.91	1954.7	13.1	1.35	0.440	74	9.2	59.8	0.6	MS
153	703- 72	23 47	53.756	-4	55 54.37	1954.6	14.4	0.96	0.199	178	8.1	182.8	0.5	SD
154		17 46	23.654	-18	6 57.04	1950.5	13.4	1.12	0.210	207	7.7	136.5	0.7	MS
155	751- 14	18 42	58.553	-11	8 41.05	1951.6	14.6	-0.17	0.354	224	10.4	71.2	0.6	WD
156		0 9	52.296	+53	1 12.89	1953.0	13.2	1.43	0.240	85	9.7	52.1	0.5	MS
157	629- 12	18 6	21.109	+2	3 21.24	1953.5	11.4	0.57	0.358	210	5.0	197.2	0.8	SD
158	256- 19	7 30	9.144	+32	48 32.45	1953.1	18.1	1.08	0.226	249	9.0	663.7	0.4	SD
159	695-496	20 31	55.817	-8	26 14.34	1951.6	17.6	0.49	0.259	62	15.3	27.9	0.6	WD
160		6 59	29.456	+19	30 43.81	1951.9	12.9	1.00	0.280	225	8.4	81.0	0.4	SD

Table 4—Continued

Event #	Name	RA h m s	DEC ' "	Epoch	V	$B-V$	μ "/yr ⁻¹	p.a.	M_V	r pc	M M_\odot	Class
161	679- 21	14 4 49.449	-5 31 20.97	1957.3	17.3	0.22	0.244	253	13.3	65.2	0.6	WD
162	329- 55	16 20 36.017	+29 15 18.05	1954.5	16.0	1.00	0.285	184	8.4	337.8	0.4	SD
163		19 31 30.369	+32 20 51.07	1951.5	14.5	1.00	0.310	341	8.4	169.3	0.4	SD
164	782- 13	7 19 21.569	-19 4 53.58	1953.0	12.9	1.20	0.192	12	8.2	86.2	0.6	MS
165	746- 41	17 0 42.977	-9 25 24.00	1950.4	15.5	0.84	0.313	225	7.2	459.0	0.5	SD
166	244- 7	1 48 42.049	+38 16 21.41	1954.7	13.6	1.20	0.276	127	10.0	52.7	0.3	SD
167	159- 34	5 57 28.351	+48 32 39.74	1953.0	15.4	0.96	0.396	169	8.1	289.7	0.5	SD
168	751- 12	18 55 11.684	-9 3 45.85	1951.6	12.8	0.84	0.332	321	7.2	132.4	0.5	SD
169	173- 45	13 41 50.647	+47 0 7.31	1956.3	16.9	1.16	0.201	282	9.6	285.4	0.3	SD
170		2 8 43.243	+25 36 23.04	1953.8	13.7	1.00	0.332	79	8.4	117.1	0.4	SD
171	80 -81	1 43 23.245	+62 39 32.99	1954.8	15.0	1.08	0.184	156	9.0	159.2	0.4	SD
172	58-151	7 20 3.997	+68 27 48.49	1953.2	18.3	1.16	0.220	223	9.6	543.8	0.3	SD
173	105-523	20 3 9.377	+61 2 39.19	1952.6	12.3	0.84	0.187	13	7.2	105.1	0.5	SD
174	757-135	21 13 8.750	-9 48 56.67	1953.7	17.0	1.20	0.181	216	10.0	252.4	0.3	SD
175	13- 86	1 3 52.689	+79 40 21.83	1954.7	14.8	0.77	0.205	83	6.5	445.0	0.6	SD
176		16 50 22.991	-1 46 17.73	1950.5	13.4	0.61	0.257	198	5.3	418.4	0.7	SD
177	119- 44	5 28 3.986	+54 55 40.67	1955.0	15.3	1.08	0.206	142	9.0	182.8	0.4	SD
178	816- 34	21 0 36.811	-18 16 44.59	1954.6	17.2	0.92	0.198	207	7.8	750.2	0.5	SD
179	196- 61	2 25 29.837	+44 47 46.22	1952.0	11.9	0.65	0.204	238	5.6	185.5	0.7	SD
180	228- 28	18 7 42.209	+40 23 54.16	1951.6	18.3	1.16	0.195	227	9.6	543.8	0.3	SD
181		0 41 57.203	+57 48 4.79	1952.7	13.7	1.12	0.235	106	9.3	73.9	0.4	SD

Events are given in the order of increasing τ (see Table 5). Names are taken from NLTT. Right ascension and declination come from USNO-A2.0 (except for Event # 55 that has position from NLTT). Equinox J2000, epoch is that of the plate and is given in a separate epoch. Visual magnitude is in Tycho system, transformed from USNO-A2.0 photographic magnitudes. Color is in Johnson system, also transformed from photographic magnitudes. Proper motions are from NLTT, with equinox J2000. For distance, physical parameters and class, see § 3.1 (MS - main sequence star, SD - subdwarf, WD - white dwarf).



Nearby Microlensing Events - Identification of the Candidates for the Space Interferometry Mission

Samir Salim and Andrew Gould

Ohio State University, Department of Astronomy, Columbus, OH 43210
E-mail: samir@astronomy.ohio-state.edu, gould@astronomy.ohio-state.edu

ABSTRACT

The *Space Interferometry Mission (SIM)* is the instrument of choice when it comes to observing astrometric microlensing events where nearby, usually high-proper-motion stars (“lenses”), pass in front of more distant stars (“sources”). Each such encounter produces a deflection in the source’s apparent position that when observed by *SIM* can lead to a precise mass determination of the nearby lens star. We search for lens-source encounters during the 2005-2015 period using Hipparcos, ACT and NLTT to select lenses, and USNO-A2.0 to search for the corresponding sources, and rank these by the *SIM* time required for a 1% mass measurement.

For Hipparcos and ACT lenses, the lens distance and lens-source impact parameter are precisely determined so the events are well characterized. We present 36 candidates beginning with a 61 Cyg A event in 2012 that requires only a few minutes of *SIM* time. Proxima Centauri and Barnard’s star each generate several events. For NLTT lenses, the distance is known only to a factor of 3, and the impact parameter only to 1”. Together, these produce uncertainties of a factor ~ 10 in the amount of *SIM* time required. We present a list of 181 NLTT candidates and show how single-epoch CCD photometry of the candidates could reduce the uncertainty in *SIM* time to a factor of ~ 1.5 .

Subject headings: astrometry – Galaxy: stellar content – gravitational lensing – stars: fundamental parameters (masses)

1. Introduction

One is used to thinking of microlensing events as taking place towards the Magellanic Clouds or the Galactic bulge. In both of these cases the lens is a faraway object, either a star belonging to the same system as the source star (self-lensing), a distant star in the Milky Way’s disk, or a member of Milky Way’s halo (whatever its nature might be). The effect that is routinely observed in such cases is the change in source’s brightness, but also present is an additional effect of the deflection of the source apparent position (Boden, Shao & Van Buren 1998). The deflection is so small ($\sim 100\mu\text{as}$) as to be unobservable with present-day facilities. However the unprecedented astrometric precision of the *Space Interferometry Mission (SIM)* ($4\mu\text{as}$) will enable such measurements.

SIM will also make possible observing microlensing events produced by *nearby* stars (“lenses”) moving in front of more distant stars (“sources”). In such cases the deflection is the only observable effect, and so the encounters are referred to as *astrometric* microlensing events. Astrometry of such an event would yield the *mass* of the lens, i.e., the nearby star. Indeed this is the only known method to obtain the masses of stars not residing in binary systems. Initially proposed by Refsdal (1964), this idea was later examined by Paczyński (1995, 1998) and Miralda-Escudé (1996) in the context of rapid developments in space-based astrometry. Gould (1999) quantified the *SIM* time required to achieve a given precision of mass measurement (say $\sigma_M/M = 1\%$) and investigated how the number of such measurements that could be made in a fixed *SIM* time depends on the characteristics of the search catalogs. The types of stars whose mass can be determined in this way will be discussed in § 5.

This paper can be seen as a direct answer to the question posed in § 4 of Gould (1999) about what can be done to identify candidates using existing catalogs. We implement the suggestions given in that section (many attributable originally to I. Reid 1999, private communication) and expand on them to produce more accurate predictions. Specifically, we search for candidate events where a lens from a proper motion catalog [Hipparcos (ESA 1997), ACT (Urban et al. 1998b), NLTT (Luyten 1979, 1980, Luyten & Hughes 1980)] passes in front of a source from the USNO-A2.0 (Monet 1998) catalog. The features of these catalogs pertinent to candidate identification are discussed in the following section. Section 3 is devoted to a treatment of the estimate of the *SIM* time required for any of these candidate astrometric microlensing events in light of the limitations of the catalogs, in particular the absence of direct distance information in most cases. In § 4 we discuss how we conducted the search for events and the extent to which we were able to overcome the various problems we encountered. In section § 5 we present lists of candidate events that we decided are real, based on the positive identification on either DSS or paper edition

of POSS I. We also discuss the features of these events in general.

2. Characteristics of the Catalogs

Our overall plan is to search for astrometric microlensing events (or ‘events’, for short) and rank these by the amount of *SIM* time required to measure the lens mass to a fixed fractional error of 1%. To this end, we would like to consult a catalog containing the positions, parallaxes, proper motions, and magnitudes of all stellar sources in the sky. Unfortunately, there is no such catalog. To understand how to make use of existing catalogs, we review the basic requirements of the search.

First, while in principle the event depends on the relative proper motion of the source and lens, the lenses, being closer, almost always move much faster in the sky than the sources. Hence, no proper-motion information is required for the sources in order to select candidate events. The USNO-A2.0 all sky astrometric catalog, which is constructed from two photographic surveys [Palomar Observatory Sky Survey I (POSS I) for $\delta > -17.5^\circ$ (‘north’ celestial hemisphere) and UK Science Research Council SRC-J survey plates and European Southern Observatory ESO-R survey plates (SERC/ESO) for $\delta < -17.5^\circ$ (‘south’ celestial hemisphere)] is therefore a nearly ideal catalog for sources, containing 526 million entries. To be included in the catalog, a star had to be detected on both the blue and red plates within a $2''$ coincidence radius aperture. Hence the catalog begins to lose completeness at $V \sim 19$ as stars fall below the detection threshold on one plate or the other. The catalog is also incomplete at bright magnitudes ($V \lesssim 11$) because of poor astrometry of saturated stars, although for these stars USNO-A2.0 contains inserted entries from the ACT or Tycho (ESA 1997) catalog. However, the epoch of these additional entries is 2000.0 and 1991.25 respectively, unlike the epoch of the other sources which is the mean epoch of the blue and the red plates (1950s for POSS I, and 1980s for SERC/ESO). In addition, USNO-A2.0 is by and large missing the stars with proper motions $\mu \gtrsim 250 \text{ mas yr}^{-1}$ in the ‘south’, because the blue and red plates of the SERC/ESO survey were on average taken 8 years apart, and so stars with $\mu > 250 \text{ mas yr}^{-1}$ moved outside the $2''$ error circle between the blue and red exposures. In reality, the time elapsed between the two plates varies from 0 to 15 years, leading to different cutoffs for each plate. This problem does not affect POSS I because its blue and red plates were taken on the same night. Neither the incompleteness at bright magnitudes nor the incompleteness at high proper motions has any significant effect on USNO-A2.0 as a catalog for microlensing *sources*, since they are usually faint and move very slowly. However, both have substantial impact on our efforts to obtain critical information from this catalog about the *lenses* (see below).

The *relative* position errors, important for NLTT events, for USNO-A2.0 are about 150 mas. For Hipparcos and ACT events, it is the absolute errors [USNO-A2.0 uses ICRS (International Celestial Reference System) as its reference frame] of about 250 mas that are relevant. There is, of course, an additional error in the position of the *source* in 2010 due to 60 years of proper motion in the case of POSS I and 30 years for the SERC/ESO plates. Since typical sources are on average 3 kpc distant and are moving at 25 km s^{-1} in each direction, this gives a proper motion of $\sim 2 \text{ mas yr}^{-1}$. This proper motion adds about 100 mas in the ‘north’ and 50 mas in the ‘south’ to the total positional error. Hence, the total error on average is about 170 mas (260 mas in the absolute system). Note that this will not be improved significantly by the release of the USNO-B all-sky position and proper motion catalog (D. Monet 1998, private communication), since its proper-motion errors will be of the same order as the proper motions of typical source stars. USNO-B will be compiled by comparing first generation sky surveys with the second generation. The absolute photometry errors in USNO-A2.0 are said to be about 0.25 mag for the stars that are not saturated. USNO-A2.0 lists photographic blue and red magnitudes. The equinox of the coordinates is ICRS J2000.

The probability p that any individual lens will deflect light from a more distant star enough to measure the lens mass M to fixed fractional accuracy is

$$p \propto N_s \pi \mu M, \quad (1)$$

where N_s is the surface density of sources, and π and μ are the parallax and proper motion of the lens. One therefore expects events to be clustered near the Galactic plane, and for nearby, fast-moving stars to be over-represented as lenses. However, there are a greater number of distant than nearby stars and consequently more stars with low than high proper motions. The net of these two competing effects is that for parallax-limited and proper-motion-limited catalogs, the total number of events scales as (Gould 1999)

$$N_{\text{events}} \propto \pi_{\text{min}}^{-1}, \quad N_{\text{events}} \propto \mu_{\text{min}}^{-1}, \quad (2)$$

where π_{min} and μ_{min} are the limits of the respective types of catalogs of lenses. Of course, the total number of potential lenses that one must examine scales as π_{min}^{-3} or μ_{min}^{-3} . Thus it is most efficient to start with high π or high μ stars and move progressively to more distant or slower ones. In practice, one has available magnitude-limited and not distance-limited catalogs, but for stars of fixed absolute magnitude these are effective distance-limited.

We search for lenses in three catalogs, Hipparcos, the ‘ACT Reference Catalog’ (ACT) and the ‘New Luyten Catalogue of Stars with Proper Motions Larger than Two Tenths of an Arcsecond and First Supplement’ (NLTT). The three catalogs have substantially different characteristics.

Hipparcos is a heterogeneous catalog with 118,000 entries. However, it has two approximate completeness characteristics that are very useful for understanding its role in the present study. First, it is approximately complete for $V < 8$, with 41,000 stars to this limit. Second, it contains essentially all the NLTT stars brighter than its operational limit of $V \sim 12$. As we mention below, NLTT is nominally complete for $\mu > 180 \text{ mas yr}^{-1}$. Based on statistical tests of the Hipparcos catalog, we find that it (and thus presumably NLTT) is essentially complete for $\mu > 220 \text{ mas yr}^{-1}$ and $V < 11$. In its last magnitude ($11 < V < 12$), Hipparcos shows some evidence for incompleteness, perhaps because of the difficulty of making precise conversions from NLTT’s photographic magnitudes to the near-Johnson system used by Hipparcos. There are 6500 Hipparcos stars with $\mu > 200 \text{ mas yr}^{-1}$ and 15,000 with $\mu > 100 \text{ mas yr}^{-1}$.

Hipparcos stars have trigonometric parallaxes with typical precisions of 1 mas. As we discuss in § 3, uncertainty in the distance to the lens is the main problem in estimating the amount of *SIM* time required for a lens mass measurement. This uncertainty is virtually eliminated for Hipparcos stars. In addition, we use Hipparcos parallaxes to calibrate our method for estimating distances of stars in the other two catalogs which lack trigonometric parallaxes. Hipparcos positions are accurate to 1 mas, while the proper motions have errors of order 1 mas yr^{-1} , implying an error of about 20 mas in the star’s 2010 position. This is negligible compared to the error in the source position given in USNO-A2.0. Finally, most Hipparcos stars have Tycho photometry which is accurate to of order 0.01 mag. Even those stars lacking Tycho photometry usually have ground-based photometry of similar quality. Tycho photometry is far better than the minimum precision required for the present search.

The ACT catalog is constructed by matching stars common to both the Astrographic Catalogue 2000 (AC 2000, Urban et al. 1998a) and Tycho with epochs circa 1910 and 1990 respectively. Such a long baseline combined with Tycho’s precise positions, permits the proper motion accuracy of ACT to be $\sim 3 \text{ mas yr}^{-1}$ (ten times better than Tycho itself). ACT is the largest (nearly 1 million stars) all-sky catalog containing proper motions. It is limited at the faint end by incompleteness of the Tycho catalog which sets in over the range $11 \lesssim V \lesssim 11.5$, and at the bright end by incompleteness (due to saturation) of plates that produce AC 2000. Completeness of ACT with respect to Tycho (entries that have proper motion) is about 95% in the $6 < V < 12$ range, and drops to 50% for $V \sim 3$. There is also a cutoff at high proper motions ($\mu \gtrsim 1.''5 \text{ yr}^{-1}$), which results from the lack of proper-motion information about these stars in the Tycho catalog. Typical errors of ACT proper motions imply an uncertainty in 2010 position of about 60 mas. This is still small compared to the uncertainty of the source position and so can be ignored. Tycho photometry is available for the great majority of ACT stars and, as stated above, this has much higher precision than is required for the present study. As we discuss in § 5.1, we are able to estimate the

distances to ACT stars with $\sim 30\%$ accuracy which is quite adequate for our purposes.

NLTT is nominally complete to $\mu > 180 \text{ mas yr}^{-1}$ and $V < 18$ (see discussion in § 5.) NLTT α and δ are given only to 1 s and 0.1' respectively (in some cases to 0.1 min and 1' respectively) and so are not sufficiently accurate to predict lens-source encounters which typically have impact parameters $\beta \sim 1''$. Hence to obtain improved positions we search for the corresponding entries in USNO-A2.0. Recall that USNO-A2.0 entries have position errors of 250 mas. However, recall also that in the ‘south’ ($\delta < -17.5^\circ$) USNO-A2.0 is missing a large fraction of the NLTT stars. To recover this part of the NLTT catalog, it would be necessary to make new position measurements for the majority of NLTT stars in the ‘south’, or at least for all that pass within $6''$ (position error of NLTT) of some source star. This would be a major project which we do not attempt. Reid (1990) finds that proper motion errors in NLTT are typically 20 mas yr^{-1} at the faint end. By comparing NLTT and Hipparcos, we find a similar value at the bright end. When this is propagated over a 60 year baseline (the epoch of NLTT is circa 1950), it implies errors of $1.2''$ in 2010 position. This is the dominant astrometric error for these stars and has important consequences as we discuss in § 3.2 below.

Because NLTT stars must be found in USNO-A2.0 in order to be used, they automatically have available two sources of photometry, both photographic. As we discuss in § 3.1, it is necessary to transform these photographic systems to the Johnson-like system used by Tycho in order to estimate distances. We find that the transformation from USNO-A2.0 colors to Johnson $B - V$ has somewhat smaller scatter than the transformation from NLTT colors, and we therefore use the former. This scatter (0.24 mag) is still substantially larger than we would like. As we discuss in § 3.1, it leads to a factor 1.7 uncertainty in distance estimates for NLTT stars.

In brief, Hipparcos alone may be roughly thought of as complete for $V < 8$ and for $\mu > 180 \text{ mas yr}^{-1}$ and $V < 12$. ACT is roughly complete for $V < 12$. Thus, the combination of Hipparcos and ACT (which both have high quality proper motions and distance estimates) is approximately complete for $V < 12$. This sample is complemented by NLTT which is roughly complete for $V < 18$ and $\mu > 180 \text{ mas yr}^{-1}$, but has much lower quality proper motion and distance estimates.

There is one important additional source of incompleteness. Suppose that a lens will pass close to a source in 2010 with a relative proper motion μ . The source must be identified from USNO-A2.0 which is based on plates taken $\delta t \sim 60 \text{ yr}$ earlier for the ‘north’ and $\delta t \sim 20 \text{ yr}$ earlier for (the later of the two plates in) the ‘south’. At this time, the lens and source will be separated by $\mu \delta t$. If the lens is sufficiently bright, it will appear as a blob on the photographic plates and will therefore “blot out” the source at the epoch of the plate,

and so the source will not appear in USNO-A2.0. The exact blot-out radius depends on the magnitude of both the lens and the source (fainter stars will get blotted-out farther from the lens). However, the great majority of sources are relatively faint ($V \sim 17$). For simplicity, we therefore identify this radius as a function of lens magnitude, $\theta(V)$, the point where 50% of $V \sim 17$ stars are lost. We find for $V = 2, 5, 8, 11, 15$ that $\theta(V) = 350, 80, 21, 11, 4$ arcseconds respectively. Thus, for example, for a $V = 8$ lens (i.e., $\theta = 21''$), the minimum proper motion required to allow an event to be detected is $\mu_{\min} = \theta(V)/\delta t = 350 \text{ mas yr}^{-1}$ in the ‘north’ or 1000 mas yr^{-1} in the ‘south’.

3. Error Triage

The basic requirement for constructing a list of astrometric microlensing events is to rank order the events by the amount of telescope time (here specifically *SIM* time) needed to make a mass measurement of a specified precision. At a later stage, one might decide to eliminate events with short observation times because of some difficulty in carrying out the observations, and one might choose to skip down the list to include an event with a long observation time because the lens in question is exceptionally interesting. However, in this paper we will be concerned primarily with the fundamental requirement of rank ordering the events.

The observation time needed for a 1% mass measurement is given by (Gould 1999)

$$\tau = T_0 \alpha_0^2 \left(\frac{r \beta c^2}{4GM} \right)^2 10^{0.4(V_s - 17)} \gamma \left(\frac{\mu t_0}{\beta}, \frac{\mu \Delta t}{\beta} \right), \quad (3)$$

where r is the distance to the lens, β is the impact parameter of the event (the projected angular separation at the time t_0 of closest approach), M is the mass of the lens, V_s is the apparent magnitude of the source, μ is the relative lens-source proper motion, $\Delta t (= 5 \text{ yr})$ is the duration of the experiment, γ is a known function which is discussed in detail by Gould (1999), $T_0 = 27$ hours, and $\alpha_0 = 100 \mu\text{as}$.

In order to estimate τ , one must first measure or estimate r, β, M, V_s, μ , and t_0 . Of course, there will be errors in all of these quantities, and these will in turn generate errors in τ . In most cases, these errors can be reduced by making additional observations or carrying out additional investigations of various types. However, these refinements often require substantial legwork. Therefore, one should first decide what is an acceptable level of error in τ and what are the main contributors to it.

The event catalog will be constructed in three stages. Stage 1 is an automated search of a pair of star catalogs (sources and lenses) for events with estimated observation times

$\tau \leq \tau_{\max,1}$. Stage 2 is a simple (but potentially very time consuming) check of this list to eliminate spurious candidates. In stage 3, additional observations are made of the remaining candidates. The estimate of τ is refined and the final list is constructed with a more restrictive maximum observation time $\tau \leq \tau_{\max,3}$, and $\tau_{\max,3} < \tau_{\max,1}$.

What level of errors are acceptable at stage 1 and stage 3? At the outset it should be emphasized that errors in the estimate of τ do not cause errors in the final mass measurement by *SIM*. The cost of errors in stage 3 is that the *SIM* observations will be too short (causing larger than desired statistical errors in the mass measurement) or too long (wasting valuable *SIM* time pushing down the mass measurement errors below what is actually desired). Hence, a factor of two error is acceptable. That is, if the *SIM* time were underestimated by a factor of 2, then the mass-measurement error would be 1.4% instead of 1%. This would be a bit worse than desired but on the other hand there would be a saving of *SIM* time that could be applied to other stars. If the *SIM* time were overestimated by a factor of 2, then one would waste some *SIM* time on the event, but one would reduce the error to 0.7% which is not completely without value. On the other hand, factor of 10 errors are not acceptable. Either one would waste a huge amount of *SIM* time or one would obtain a mass measurement with an error much larger than desired. As a corollary, errors that are small compared to a factor of 2 can be ignored at any stage.

Much larger errors can be tolerated at stage 1 than stage 3. For example, if the stage-1 estimates could be in error by a factor of 10, then one must set $\tau_{\max,1} = 10\tau_{\max,3}$ to avoid losing viable candidates. The cost is that the candidate list is increased by a factor $(\tau_{\max,1}/\tau_{\max,3})^{1/2} \sim 3$ (Gould 1999), and one must then sift through this larger list in stages 2 and 3. Clearly, however, this work load can become prohibitive for sufficiently large errors.

We now show that of all the input parameters, only the distance r and the impact parameter β can induce sufficiently large uncertainties in τ to warrant special attention. We examine the various parameters in turn.

If the lens is taken from the Hipparcos catalog, it will have a trigonometric parallax. In virtually all cases of interest, the lens will be close enough ($r \lesssim 200$ pc) that the distance error will be less than 20%, which is quite adequate for present purposes. If the lens does not have a trigonometric parallax, its distance must be estimated from its measured flux (in say V band) F_V together with an estimate of its intrinsic luminosity, L_V :

$$\tau \propto r^2 = \frac{L_V}{4\pi F_V}. \quad (4)$$

Equation (4) makes it appear as though the uncertainty in τ will be enormous. For example, a star with a measured color $V - I = 1$ could plausibly be a clump giant with $M_V = 1$, a main-sequence star with $M_V = 6$, a subdwarf with $M_V = 8$, or a white dwarf

with $M_V = 14$. This covers a range of 1.6×10^5 in luminosity and implies an uncertainty in τ of the same magnitude. Nevertheless, we will show in § 3.1 that with good photometry, r can be determined with $\sim 30\%$ accuracy which implies an error in τ of less than a factor of 2. Stars in the ACT catalog have good (Tycho) photometry. For stars in NLTT only photographic photometry is generally available. We will show in § 3.1 that for NLTT the 1σ errors in L_V (and so τ) are a factor of 3.

As discussed in § 3.1, the first step in estimating the distance to the lens is to determine its luminosity class (e.g., white dwarf, subdwarf, main-sequence, or giant star). If this is properly determined, then the lens mass can be estimated quite accurately from the color. For the cases where the luminosity class is not correctly determined, the error induced in the distance is much greater than the error induced in the mass. Thus, in either case, the error in the mass can be ignored.

The geometry of the event (μ , β , and t_0) is determined from the astrometry. These quantities affect the estimate of τ through the β^2 factor and the γ factor in equation (3). We focus first on the β^2 factor. As discussed in § 2, the relative source-lens position error (and hence the error in β) is about 260 mas for lenses in Hipparcos and ACT and about $1''.2$ for NLTT. In § 4, we discuss how these errors are incorporated into the search procedure.

According to equation (3) the 0.25 mag error in the source magnitude from USNO-A2.0 induces a 25% error in τ . We ignore this.

Finally, since the launch date of *SIM* is not fixed, we do not attempt to calculate γ based on the time of closest approach t_0 relative to the midpoint of the mission, $\gamma(\mu t_0/\beta, \mu\Delta t/\beta)$. Rather, we calculate γ for the optimal possible launch date for the given event when the midpoint of the mission coincides with the time of closest approach, i.e., $t_0 = 0$. That is, we use $\gamma(0, \mu\Delta t/\beta)$. Some representative values are $\gamma(0, x) = 10$ for $x \geq 4$, $\gamma(0, 2) = 19$, and $\gamma(0, 1) = 99$. When the launch date is fixed, one can substitute the correct first argument in place of 0. In some cases, γ may rise significantly but in others (particularly when $\mu\Delta t \gg 4\beta$) it will hardly be affected. In any event, because we are suppressing consideration of the first argument, any uncertainty in t_0 does not enter our calculation.

3.1. Lens Distances

Here we describe our method for estimating the distances to the lenses and evaluate the accuracy of these estimates. Our method has three distinct steps. First, we assign a luminosity class to each star based on its position in a reduced proper-motion diagram.

Second, we assign a V band luminosity L_V (equivalently M_V) to each star based on its luminosity class and color. Third, we combine the L_V with the measured flux from the star F_V (equivalently V) to obtain a distance. We apply the method to both the ACT and NLTT catalogs. However, to calibrate and describe the method, we first apply it to Hipparcos stars with parallax errors smaller than 20%. After the method is calibrated, we use it to “predict” the distances to these stars and then compare the results to the measured Hipparcos parallaxes.

Figure 1 is a reduced proper motion diagram of Hipparcos stars with parallax errors smaller than 20%. (Please note that throughout this paper we will use V magnitudes in Tycho system, and $B - V$ colors in Johnson system. To get Johnson magnitudes, use the transformation (ESA, 1997): $V_J = V - 0.090(B - V)$. Consequently M_V is in Tycho system as well.) If all stars had identical transverse speeds v_* , then this diagram would look exactly like a color-magnitude diagram (CMD), but with the vertical axis shifted by $5 \log(v_*/47.4 \text{ km s}^{-1})$. This means that disk stars (i.e., white dwarfs, main-sequence stars, and giants) which have typical $v_* \sim 30 \text{ km s}^{-1}$ are shifted upward by 1 mag, while halo stars (i.e., subdwarfs) which have typical $v_* \sim 240 \text{ km s}^{-1}$ are shifted downward by 3.5 mag. That is, the ~ 2 mag separation between the main sequence and the subdwarfs in a “normal” CMD is here augmented to ~ 6.5 mag. We separate luminosity classes according to the bold lines shown in the diagram. Once these classes are chosen, we assign absolute magnitudes by

$$M_V = 11.6 + 7.56(B - V) \quad (\text{white dwarfs}), \quad (5)$$

$$M_V = 0.4 + 8.00(B - V) \quad (\text{subdwarfs}), \quad (6)$$

$$M_V = 0.7 + 6.27(B - V) \quad (\text{main sequence}), \quad (7)$$

and

$$M_V = 6.0 - 4.14(B - V) \quad (\text{giants}), \quad (8)$$

for white dwarfs, subdwarfs, main-sequence stars, and giants respectively. These linear relations are obtained using the real Hipparcos color-magnitude diagram.

Figure 2 compares the distances of Hipparcos stars derived from these luminosity estimates (together with the measured V mags) to the true distances based on parallax. For the typical lens distance moduli of less than 2.7 ($r = 35 \text{ pc}$) the dispersion (excluding outliers) is 0.53 mag. This is equivalent to a distance uncertainty of 28%, and an error in the estimate of τ of 63%. For distance moduli greater than 2.7, the dispersion is larger, but this is dominated by giants which are of little practical interest in the present search.

We directly apply this technique to the ACT catalog for which there is generally excellent photometry from Tycho.

For NLTT, generally only photographic photometry is available. Because of the large position errors in the NLTT catalog, we can search for astrometric lensing events only if we can identify the NLTT star with the corresponding object in USNO-A2.0. Thus, in all cases we have photometry from USNO-A2.0. We convert from USNO-A2.0 mags to Johnson color and Tycho V using the relations

$$B - V = 0.22 + 0.39(B_{\text{ph}} - R_{\text{ph}}), \quad V = R_{\text{ph}} - 0.27 + 0.46(B_{\text{ph}} - R_{\text{ph}}), \quad (9)$$

for POSS I, and

$$B - V = 0.38 + 0.32(B_{\text{ph}} - R_{\text{ph}}), \quad V = R_{\text{ph}} - 0.05 + 0.40(B_{\text{ph}} - R_{\text{ph}}), \quad (10)$$

for SERC/ESO. The transformations were derived by comparing USNO-A2.0 with ACT (Tycho photometry), and discarding 3σ outliers. Here, B_{ph} and R_{ph} are blue and red photographic magnitudes, respectively. The scatter in the predicted versus actual $B - V$ is 0.24 mag. Since the slope of the main sequence is $\Delta V/\Delta(B - V) \sim 5$, the error in distance modulus of NLTT stars is ~ 1.2 mag or about a factor of 1.7 in distance. This corresponds to a factor 3 error (1σ) in SIM time.

In the case of ACT and NLTT, the distance is also used to find the luminosity, that in turn (using mass-luminosity relations) determines the masses of main sequence stars and subdwarfs. For giants and white dwarfs we adopt mass of $1M_{\odot}$ and $0.6M_{\odot}$ respectively.

With Hipparcos, the mass is found directly because their distances, and therefore luminosities are known from trigonometric parallax. Thus, we only need to correctly determine the luminosity type based on luminosity and color (CMD). This is fairly straightforward for giants and white dwarfs, but can be ambiguous for main sequence stars vs. subdwarfs since they occupy not too different regions of CMD. We differentiate them by their 2D-velocities, calling stars with $v > 85 \text{ km s}^{-1}$ subdwarfs. Exact classification is only possible with additional information, such as a spectrum.

3.2. Impact Parameter

At first sight, the uncertainty in the impact parameter (260 mas for Hipparcos and ACT, $1''.2$ for NLTT) would appear to wreak havoc with the estimate of τ . For example, any source whose calculated impact parameter with respect to an NLTT lens is less than $2''$ might actually pass within 50 mas or even closer, thus reducing its SIM time by a factor of 1600 or more. In essence, one would seem to be forced to do follow-up observations of all encounters in this catalog having apparent impact parameters $\beta < 2''$ in order to find the small subset with very close encounters. In fact, the situation is not quite so severe.

The size of the stop for *SIM* has not yet been fixed, but is likely to be about 300 mas. This is about the size of the envelope of the *SIM* fringe pattern (set by the 25 cm size of the mirrors). Hence, if the lens is as bright as the source then it would be difficult to obtain reliable astrometry while the source is within 300 mas of the lens. Typically, the lens will be much brighter than the source so the problem will be even more severe. For events with $\beta < 300$ mas, observations can be carried out during most of the event, but must be suspended during the period of closest approach. The precision of the mass measurement will then be approximately the same as for an event with $\beta = 300$ mas. That is, there is an effective minimum impact parameter, $\beta_{\min} = 300$ mas.

We account for the errors in distance and impact parameters as follows. We aim for a final catalog with $\tau_{\max,3} = 100$ hrs. For the Hipparcos and ACT lenses, we accept the lens distances and impact parameters at face value, but set $\tau_{\max,1} = 300$ hrs to allow for errors, primarily overestimation of the impact parameter. For NLTT we set $\tau_{\max,1} = 1000$ hrs to allow for 1σ photometry errors. In addition, we calculate the τ^* (the best-case τ) by reducing β so that

$$\beta^* \rightarrow \max(\beta - 1.''8, 0'') \quad (11)$$

We always use the reduced β^* to calculate the corresponding γ factor that enters τ^* , but in cases when $\beta^* < 300$ mas, we use $\beta^* = 300$ mas for the value of the impact parameter, because of the discussed aperture stop. Finally, we allow all events where the lens is fainter than the source and the nominal impact parameter is $\beta < 1.''8$ on the off chance that the true impact parameter is very small. It is this best-case τ^* on which we impose the 1000 hr limit. These three adjustments to the NLTT-based catalog mean that it will contain a large number of spurious candidates. These must be eliminated by follow-up observations to obtain better photometry and astrometry.

4. Searching for the candidate events

Although the basic strategy for searching for the candidate events is the same for all three catalogs (Hipparcos, ACT and NLTT) there are some specific details that apply to each of them. Also, there were certain problems associated with the raw lists of events produced by these catalogs. That is, each catalog’s initial list had its own set of ‘events’ that turned out not to be real.

The catalog of sources, USNO-A2.0, is written on 11 CD-ROMs, and the sky is divided into 24 zones each corresponding to 7.5° in declination. Each zone is written as one file. Our search program processes one zone at a time, checking every lens star that lies within that zone.

First, the initial position of the lens in J2000.0 coordinates is needed. In the case of Hipparcos and ACT this is straightforward as they both list coordinates in the ICRS J2000.0 system, the one used by USNO-A2.0. One only needs to apply proper motion in order to change the epoch of the coordinates from 1991.25 and 2000.0 (Hipparcos and ACT, respectively) to that of the search period (2005-2015). In the case of NLTT, the procedure is much more involved. First, as explained in § 2, we need to identify NLTT stars in USNO-A2.0 in order to get more accurate positions. We must therefore find a matching USNO-A2.0 star close to the position where NLTT was at the epoch of the *specific* plate that was scanned to produce entries in USNO-A2.0. This is essential because the span of plate epochs is quite wide, and the NLTT stars, having large proper motions, change their positions quickly. Therefore, in the first pass we look for anything close to where the NLTT star was at the mean epoch of entire POSS I (or SERC/ESO in the ‘south’). Since each USNO-A2.0 entry has a record of the plate from which it was scanned, we can determine the epoch from the table of plate epochs. With the exact epoch we know where precisely to look for an NLTT star. We do that by checking a $1'.5 \times 1'$ error box ($\Delta_\alpha \times \Delta_\delta$), that accounts even for the worst initial NLTT positions. We accept as the best match a USNO-A2.0 star that is closest to the predicted position and has similar magnitude and color (in cases when NLTT lacks color information, only magnitude is used). In the ‘north’, a match is found in some 90% of cases (90% of which are within $10''$ of the expected position). In the great majority of cases when there is no match, the NLTT star was too faint to pass the detection limit of USNO-A2.0, or it was too bright, and therefore USNO-A2.0 had an entry with saturated photometry. However, the bright NLTT stars are almost always recovered in Hipparcos and/or ACT. We made a special effort *not* to search NLTT stars that were included in Hipparcos or ACT: as discussed in § 2, the NLTT data are of much lower quality and would generate many spurious events that are eliminated by the better Hipparcos and ACT data. We screen for these duplicates by looking for Hipparcos stars around NLTT positions that have similar proper motions ($\Delta\mu_\alpha, \Delta\mu_\delta < 40\text{mas yr}^{-1}$), and not too different magnitudes. We find 6233 matches, i.e., most of the Hipparcos stars with $\mu > 200\text{mas yr}^{-1}$. These matches are then flagged and skipped when identifying NLTT stars in USNO-A2.0. Also, if the match in USNO-A2.0 is associated with an ACT star, such NLTT star is also skipped. Occasionally, no match for an NLTT star is found because the input position was completely wrong [most likely typos, since a machine-readable NLTT was produced by Optical Character Recognition (OCR)]. Identification efficiency is much worse in the ‘south’ (SERC/ESO) for reasons discussed in § 2. Only 20% of NLTT stars are found within $10''$ of the expected position.

Next, the basic search strategy is to produce a box, the diagonal of which represents the lens’s proper motion from 2005 to 2015, the time span in which an event should take

place. The size of the box is further increased by 5 years worth of proper motion (i.e, the largest possible impact parameter) to allow for events that take place near the starting and final years. We then find all the stars in USNO-A2.0 that are located within this box. A moving star, i.e. the lens, will pass by these stars, but not every encounter will produce a microlensing event. As discussed in § 2 and § 3 this depends on the physical parameters of the lens and on the brightness of the source star. We look for events that can be observed with $\tau_{\max,1} < 300$ hrs (1000 hrs for NLTT). For a given source star this corresponds to some maximum impact parameter β_{\max} . We ask that the impact parameter of an encounter be $\beta < \beta_{\max}$. (In the case of NLTT, we also use the reduced impact parameter β^* , as described in § 3.2) . All other encounters are discarded. Another condition an encounter must meet is $\beta < \Delta t \mu$, ($\Delta t = 5$ yr) which is needed to keep γ in equation (3) from becoming infinite.

Additionally, when searching ACT we discard encounters with stars that were labeled in USNO-A2.0 as being associated with ACT, in order to avoid finding encounters of an ACT star with ‘itself’. It might not sound logical to find an ACT star approaching its USNO-A2.0 entry in the *future*, but this happens with some slowly moving ACT stars because the astrometry of bright USNO-A2.0 stars is poor. A similar problem is present with bright Hipparcos stars, for which USNO-A2.0 sometimes contains multiple spurious entries. We discard these based on brightness and proximity of the Hipparcos star to the USNO-A2.0 entry at the epoch of the plate. Despite these automated rejection criteria, some ‘events’ that are nothing other than the lens and its entry in USNO-A2.0, make their way into a final list. This most often happens because bright stars, having bad astrometry in USNO-A2.0, produce multiple entries if located in overlapping regions of the plates. These ‘events’ are characterized by very short *SIM* observing times (because the ‘source’ magnitude is bright). We check them by hand, by looking at the sky survey images themselves and making sure that there is only one star present.

Once an event satisfying all criteria is found, its *SIM* observing time τ is computed, and the output list containing all the information about the lens, the source, and the geometry of an event is produced. We present these results in § 5. However, the computer generated list is still far from containing only genuine events. One source of spurious entries is discussed in the preceding paragraph. Another problem, which mainly plagues events found from Hipparcos and ACT, is that since stars in these two catalogs are bright, their images in sky surveys have conspicuous diffraction spikes. These spikes in turn produce spurious entries in USNO-A2.0. Thus, sometimes an encounter will be reported in cases when the source is just an artifact from a diffraction spike. When we checked all of the Hipparcos and ACT events by comparing the sky survey images with USNO-A2.0 generated star charts (<http://ftp.nofs.navy.mil/data/>), we were able to identify such occurrences. Also, since the diffraction spikes run along right ascension and declination, it was always the stars

that had their proper motion along these directions that turned out to produce spurious events.

When it comes to NLTT, the only serious problem is with the encounters in the ‘south’, because the lens identification is often spurious. These are checked by calculating how much the lens has moved between the two plates. If that distance is less than the $2''$ error circle (see § 2) the chances are greater that the lens identification, and therefore the event, are real. Since there are not many of them, we check the ‘south’ NLTT events by hand. Also, since the NLTT position is sometimes completely off, it could lead to the wrong USNO star be identified as a match for NLTT star. Such a misidentified star might even produce an ‘event’. Since we do not check entries in NLTT list by hand, a possibility exists that some entries might not be real.

As previously discussed, we try to eliminate doing NLTT stars that are present in either the Hipparcos or ACT catalogs. However, some survive our automated procedures. Therefore we check all NLTT events up to the Hipparcos/ACT detection limit and eliminate repetitions by hand. Thus, the list should contain only NLTT stars not present in the other two catalogs.

5. Events

The events produced by stars in the Hipparcos and ACT catalogs are presented in Tables 1, 2 and 3. Tables 1 and 2 list the properties of the lens stars, while Table 3 lists those of the source stars and of the events themselves. Details about specific columns are given in the table notes. The events are ordered by the required *SIM* time. There are 36 events taking place between years 2005 and 2015. Nine of them are found using both the Hipparcos and ACT catalogs (in which case the results presented are from the Hipparcos catalog), and there is one event produced by an ACT star that is not in Hipparcos, as indicated by the last column in Table 3. If an event was detected only using the Hipparcos catalog, it is because such a star is either not listed in ACT since Tycho proper motions were missing, or because it lacks photometry.

These 36 events are produced by 28 different stars. Therefore, eight entries in Tables 1 and 2 are repetitions, but we keep them in order to preserve compatibility with Table 3, i.e., the ‘Event #’. There are some notable stars among the lenses, such as Proxima Centauri (closest star), Barnard Star (highest proper motion), and the binary 61 Cyg A/B. They, together with the only white dwarf in the list (GJ 440), undergo multiple events that will both enable a more precise mass measurement and provide a check on systematics.

We classify 11 stars as subdwarfs, although some of them might be main sequence stars, and vice versa. A convenient way of presenting the types of stars that will undergo microlensing is given in Figure 3. Plotted is the classical CMD of Hipparcos catalog stars with distances known to better than 10%. Superimposed as red dots are the Hipparcos/ACT stars that produce events listed in Tables 1-3. As we see, except for a single white dwarf, the rest of the stars are uniformly distributed within the faint ($M_V > 5$) portion of the main sequence, with subdwarfs located mostly below the densest concentration of stars. The absence of stars with $M_V < 5$ is the result of blotting out, as discussed in § 2.

Although the table includes events up to $\tau_{\max} = 300$ hrs, they are concentrated towards shorter times. For example, 1/3 of events have $\tau < 16$ hrs, and 1/2 less than 70 hrs. In fact, when we investigate the number of events as a function of τ we see a behavior that is in line with the theoretical predictions of Gould (1999).

As an example, in Figure 4 we show the $8' \times 8'$ field surrounding 61 Cyg A/B as it appeared in 1951 (DSS 1/POSS I) and in 1991 (DSS 2/POSS II) (upper left and lower left panels, respectively). We can see that the pair has moved some $3.5'$ across the field. In a $2' \times 2'$ blow-up we show the region that the pair will transverse in the period 2005-2015 (from DSS 2/POSS II). The star chart (created from USNO-A2.0 data), corresponds to the $2' \times 2'$ field and has the lensed stars labeled with the number of the corresponding event in Tables 1-3.

Additional features of the set of events found with Hipparcos and ACT will be discussed later in this section, together with the events from NLTT.

Tables 4 and 5 contain data about the 181 events found in NLTT, ordered by their nominal *SIM* observing time τ . Details about the columns are given in the table notes. These tables have many more entries than the Hipparcos/ACT tables partly because of the $\tau_{\max}^* = 1000$ hr limit compared to $\tau_{\max} = 300$ hrs for Hipparcos/ACT. In fact, there are just 59 events with $\tau < 300$ hrs. That means that if we had perfect knowledge about the NLTT stars there would be approximately 60 events in such a ‘perfect’ list, but those, of course, would not necessarily be the first 60 from our present list. However, it should be noted that out of 181 events only 11 (6%) are detected in the SERC/ESO part of USNO-A2.0 which comprises 35% of the sky. Again, the nominal *SIM* observing times are concentrated toward the lower values, and the trend of the number of events vs. τ basically agrees with Gould (1999).

NLTT events are predominantly produced by stars that we classify as white dwarfs (50%) and subdwarfs (46%), which is not surprising keeping in mind that most intrinsically bright, fast-moving stars are also apparently bright and therefore already covered by

Hipparcos and ACT.

Finally, both the Hipparcos/ACT and NLTT events can be investigated in the $V - \mu$ plane. This allows us to see the characteristics of the catalogs and events combined. Figure 5 covers a wide range of visual magnitudes ($2 < V < 19.5$) exhibited by high proper motion stars. It shows a range of proper motions from $\mu = 0.''1 \text{ yr}^{-1}$ to that of Barnard’s star. The two long-dashed vertical lines show the nominal limit of the Hipparcos catalog of survey stars ($V = 8$), and the detection limit of Hipparcos non-survey stars, of Tycho, and therefore of ACT ($V = 12$). The horizontal long-dashed line is the lower limit of $\mu = 0.''18 \text{ yr}^{-1}$ for the NLTT. The lens stars that produce event, found only in Hipparcos are designated with ‘ \times ’, and the one star found only in ACT with ‘+’. Those found in both look like asterisks. In order to present more a realistic relative number of NLTT lenses, we plot only those with nominal $\tau < 300$ hrs (circles). As discussed in § 2, the blotting out of images in USNO-A2.0 limits our ability to find events moving slower than a specific value for the given lens magnitude. We plot this function $\theta(V)$ as a short-dashed line. Because of different epochs of POSS I and SERC/ESO these cutoffs will be different in the two parts of the sky. The lower line corresponds to ‘north’ (POSS I). The region below these two lines is therefore excluded, and we can see that none of the lens stars is found there. The exclusion due to blot-out approximately follows the diagonal line corresponding to a star with $M_V = 8$, $v = 30 \text{ km s}^{-1}$. This shows that our survey cannot find disk-star lenses with $M_V < 8$, unless they are moving faster than average. Indeed, as shown in Figure 3, we find no lenses with $M_V \lesssim 5$. However, halo stars with $M_V = 8$, $v = 240 \text{ km s}^{-1}$ (upper diagonal line), are comfortably away from this limit.

6. Conclusion

Gould (1999) stressed the necessity of finding astrometric microlensing candidates to be observed by *SIM* as soon as possible, since the separation between the lens and the source is steadily getting closer, and it will become harder to produce a valid estimate of the likelihood of an event the longer we wait. With the currently available catalogs, we were able to produce a fairly reliable list of candidates from Hipparcos and ACT catalogs. However, obtaining a list of similar quality of NLTT candidates requires additional astrometric and photometric observations of the candidates in our list. A one-meter class telescope with a CCD is adequate for such a job, since NLTT stars are relatively bright. Also, since obtaining an accurate color is much more critical than a precise magnitude, the required observations can be successfully carried out in partially photometric conditions.

Another issue is getting more candidates. This can only be assured with new catalogs

of proper motions, having lower proper motion cutoffs and going to fainter magnitudes. The biggest such project is USNO-B which should list the proper motions of basically all the stars in POSS I/SERC/ESO. Having a lower proper motion limit is particularly important in $V > 12$ range, where the blotting of stellar images no longer presents a limitation (at least not in the northern hemisphere), and where NLTT goes only to $\mu = 180 \text{ mas yr}^{-1}$. USNO-B will also push the detection limit ~ 1 mag fainter compared to NLTT. Since in USNO-B all the stars will have proper motions, the uncertainty of the source star's position will also be reduced. Also, the completeness of NLTT at the fainter magnitudes is not altogether clear. According to I. Reid (1999, private communication) it is actually only about 50% complete near its proper-motion and magnitude limits. We did our own check by comparing the number of entries having $\mu > 200 \text{ mas yr}^{-1}$ in magnitude bin V with the number of entries with $\mu > 400 \text{ mas yr}^{-1}$ in magnitude bin $V - 1.5$. In a perfectly complete catalog, the ratio of these two numbers should be 8 in each bin. We see a significant drop only at $V > 18$, i.e. we find NLTT to be complete. With USNO-B this matter will most probably be resolved.

Acknowledgements: We thank I. N. Reid for valuable discussions. This research was supported in part by grant AST 97-27520 from the NSF and in part by grant NAG5-3111 from NASA.

REFERENCES

- Boden, A. F., Shao, M. & Van Buren, D. 1998, *ApJ*, 502, 538
- ESA, 1997, *The Hipparcos and Tycho Catalogues*, SP-1200
- Gould, A. 1999, *astro-ph/9905120*
- Luyten, W. J. 1979, 1980, *New Luyten Catalogue of Stars with Proper Motions Larger than Two Tenths of an Arcsecond* (Minneapolis: University of Minnesota Press)
- Luyten, W. J. & Hughes, H. S. 1980, *Proper Motion Survey with the Forty-Eight Inch Schmidt Telescope. LV. First Supplement to the NLTT Catalogue* (Minneapolis: University of Minnesota)
- Miralda-Escudé 1996, *ApJ*, 470, L113
- Monet, D. 1998, *BAAS*, 193, 120.03
- Paczyński, B. 1995, *Acta Astron.*, 45, 345
- Paczyński, B. 1998, *ApJ*, 494, L23
- Reid, N. 1990, *MNRAS*, 247, 70
- Refsdal, S. 1964, *MNRAS*, 128, 295
- Urban S. E., Corbin T. E. & Wycoff G. L. Martin, J. C. Jackson, E. S. Zacharias, M. I. 1998a, *AJ*, 115, 1212
- Urban, S. E., Corbin, T. E. & Wycoff, G. L. 1998b, *AJ*, 115, 2161

Fig. 1.— Reduced proper motion diagram for Hipparcos stars with $\sigma_\pi/\pi < 20\%$. To avoid clutter, every 10th star is plotted. Abscissa is Johnson $B - V$ color as usually determined from Tycho photometry but sometimes from ground-based photometry. Ordinate is apparent magnitude (Tycho V) augmented by the five times the logarithm of the proper motion in units of $"\text{yr}^{-1}$. If all stars had the same transverse speed, this figure would look like an ordinary CMD. Dashed lines show median tracks of white dwarfs, main-sequence stars, and giants moving at typical disk transverse speeds of 30 km s^{-1} , and subdwarfs moving at typical halo transverse speeds of 240 km s^{-1} . Solid lines indicate the boundaries of our assignment of stars to one of these four classes.

Fig. 2.— Distance-modulus errors versus distance modulus for the Hipparcos stars shown in Fig. 1. The distance-modulus of each star is estimated by first classifying according to the bold-line divisions in Fig. 1 and then assigning it an absolute magnitude using equations (5)–(8) which form the basis for the dashed lines shown in Fig. 1. The distance-modulus error is then the difference between this estimate and the value based on the measured trigonometric parallax. For distance moduli less than 2.7, the typical errors are only $\sim 0.53 \text{ mag}$. Errors are larger for more distant stars, but these are dominated by giants which are not relevant in the present study.

Fig. 3.— A color-magnitude diagram of Hipparcos stars with distances measured to better than 10%. The event-producing stars (lenses) from the Hipparcos and ACT catalogs are superimposed in red.

Fig. 4.— $8' \times 8'$ fields around 61 Cyg A/B in 1951 (upper left panel) and 1991 (lower left panel). Shown magnified is a $2' \times 2'$ region where events will take place during 2005-2015 period. The chart corresponds to the $2' \times 2'$ field with source stars labeled with the numbers corresponding to ‘Event #’ in Tables 1-3. Events 5 and 25 are produced by 61 Cyg B, and the other four by 61 Cyg A.

Fig. 5.— Apparent magnitude - proper motion ($V - \mu$) plane showing lenses found in Hipparcos (\times), ACT ($+$) or both ($*$) catalogs. NLTT events are shown as circles. Vertical long-dashed lines are completeness limits for Hipparcos and ACT. Horizontal long-dashed line is NLTT proper-motion cutoff. Short dashed lines delineate regions excluded due to blot-out (lower line - POSS I, upper line SERC/ESO). Solid lines represent an $M_V = 8$ star at various distances if belonging to disk population (lower line) or halo population (upper line).

Table 5. NLTT - source star and event properties

Event #	RA h m s o	DEC ' "	V	$B-V$	τ hr	τ^* hr	d_{2000} "	t_0 yr	β mas
1	18 39 26.908	+4 11 34.36	15.8	0.80	0.1	0.0	3.3	2006.4	643
2	6 21 24.415	+9 38 3.81	17.9	0.73	0.5	0.5	4.4	2011.1	286
3	7 13 4.796	+33 32 13.35	17.5	0.69	0.8	0.2	5.1	2014.0	589
4	18 17 48.180	+23 17 51.85	17.1	0.81	1.0	0.1	5.0	2010.7	858
5	8 11 58.444	+8 45 29.77	18.2	0.57	1.1	0.1	54.6	2010.5	2739
6	17 36 11.180	+23 48 22.92	18.0	0.61	1.7	0.0	1.2	2006.3	139
7	20 27 29.604	-13 17 52.60	17.1	0.26	1.8	0.0	2.4	2006.5	97
8	20 48 10.791	+12 4 7.47	17.1	0.69	1.9	0.3	2.2	2009.7	552
9	6 14 16.561	-23 10 27.87	16.0	0.22	2.0	0.1	5.7	2014.6	1014
10	16 6 35.796	+24 28 36.67	18.9	0.34	2.1	2.1	4.7	2014.9	29
11	19 57 10.618	+57 52 3.30	17.4	0.42	2.5	0.3	3.0	2008.3	747
12	7 50 15.484	+7 11 15.25	16.5	0.45	2.6	0.5	23.0	2012.9	677
13	11 24 12.472	+21 21 39.63	13.6	0.65	3.3	0.2	7.2	2006.2	3094
14	19 56 29.049	-1 2 42.41	14.9	0.61	4.6	0.1	11.7	2014.7	1845
15	4 30 53.742	+28 11 49.00	16.4	0.88	5.1	0.0	7.3	2006.9	1389
16	1 16 30.439	+24 19 28.75	14.8	0.65	5.6	1.8	15.7	2007.3	8198
17	0 35 54.579	+52 41 10.83	15.4	0.49	5.6	5.6	11.7	2014.8	292
18	17 0 41.714	-18 44 30.61	18.1	0.99	6.1	0.2	5.1	2012.0	1096
19	16 1 48.023	+30 30 44.80	16.4	0.26	6.9	0.0	2.3	2010.4	504
20	20 19 4.666	+12 34 51.03	16.0	0.65	7.0	1.0	13.9	2010.8	4806
21	2 25 41.586	+42 27 5.98	18.2	0.81	7.3	7.3	2.4	2010.3	136
22	2 31 56.861	-8 32 7.50	14.8	0.65	8.0	0.0	4.3	2014.2	62
23	20 43 21.096	+55 21 11.34	18.8	0.49	11	2.1	23.9	2012.3	3761
24	17 46 36.062	-12 58 23.32	18.0	0.42	13	0.2	7.1	2009.8	2269
25	7 13 41.230	-13 28 7.39	18.4	0.45	19	1.3	14.6	2011.2	2623
26	5 10 31.269	+31 17 30.95	18.8	0.53	20	1.9	4.0	2005.7	958
27	20 14 44.983	+61 46 37.83	18.5	0.61	21	0.4	7.3	2010.2	1608
28	21 0 36.351	-18 16 53.76	15.6	0.32	24	0.0	1.3	2005.7	699
29	19 9 56.091	-13 30 37.00	18.0	0.10	25	1.5	3.7	2010.5	877
30	23 18 6.898	+49 28 12.50	14.3	0.30	26	26	1.7	2005.2	201
31	15 35 21.364	+13 6 48.03	18.5	0.34	31	0.7	3.4	2011.3	1007
32	1 9 3.653	-10 42 13.89	18.6	0.49	38	38	2.4	2012.1	196
33	4 31 12.144	+58 58 47.82	17.2	0.49	42	15	23.1	2009.2	7577
34	5 50 24.507	+17 19 11.31	18.2	0.69	42	7.0	8.6	2014.6	735
35	13 24 27.722	-33 16 26.44	18.9	1.47	49	0.4	5.1	2006.9	2048
36	19 3 14.966	-13 34 17.85	15.2	0.53	53	6.8	7.6	2007.2	5161
37	6 37 21.748	-18 58 58.92	18.9	0.99	54	10	2.6	2013.5	483
38	13 38 13.499	-2 51 3.37	16.2	0.69	71	37	33.8	2008.5	12202
39	9 17 45.018	+58 25 14.47	16.9	0.42	72	15	10.8	2007.7	6346
40	0 44 1.323	+75 12 21.47	15.9	0.88	77	0.0	3.7	2011.8	927
41	21 7 53.827	+59 43 13.82	18.2	0.61	100	37	14.2	2005.2	9104
42	9 50 43.254	-12 16 35.14	15.7	1.23	110	0.4	4.0	2009.2	2493
43	8 14 36.325	-8 1 31.87	16.7	0.38	110	0.1	4.6	2012.8	2061
44	23 6 22.537	+65 3 28.91	16.0	1.47	120	120	3.1	2009.5	40
45	1 10 44.424	+27 58 14.89	16.1	0.88	130	0.3	2.7	2009.8	1459
46	19 38 48.731	+35 12 44.24	15.3	1.00	130	130	7.7	2009.8	58
47	19 21 38.138	+20 51 49.71	18.1	1.23	150	150	15.5	2008.9	167
48	18 6 31.381	-30 9 52.44	17.4	0.58	180	35	1.6	2006.0	537
49	5 28 24.683	+39 44 58.24	13.9	0.88	180	0.3	2.6	2005.1	2350
50	22 36 36.874	+53 3 6.66	17.3	0.42	180	150	1.9	2007.3	330

Table 5—Continued

Event #	RA				DEC		V	$B-V$	τ hr	τ^* hr	d_{2000} "	t_0 yr	β mas
	h	m	s	o	'	"							
51	23	5	16.976	+71	23	13.34	17.4	0.49	190	0.0	2.8	2010.1	425
52	11	24	8.204	+35	47	31.75	19.3	0.42	190	2.5	2.9	2009.8	1120
53	22	1	8.548	+29	9	37.00	17.0	1.00	200	1.1	5.8	2009.1	2063
54	17	55	48.681	-7	36	1.15	17.8	0.88	200	200	3.2	2012.6	113
55	8	55	23.917	-4	3	32.53	15.3	0.57	230	3.9	5.9	2012.1	3107
56	16	34	18.488	+57	9	59.08	16.6	0.42	240	56	21.4	2013.2	621
57	20	43	19.242	+55	21	10.84	17.8	0.61	250	95	18.7	2008.3	10008
58	23	57	50.924	+19	49	8.43	19.3	0.49	250	6.4	3.9	2012.2	1019
59	5	38	15.351	+79	30	15.77	14.3	0.73	280	31	14.6	2011.8	3887
60	18	2	31.577	+5	44	38.71	14.5	0.96	310	0.1	4.5	2008.7	1866
61	21	35	18.521	+46	33	17.42	15.9	0.61	320	1.4	3.7	2006.3	2263
62	21	35	18.521	+46	33	17.42	15.9	0.61	320	1.4	3.7	2006.3	2263
63	3	43	54.491	+63	39	48.87	18.1	0.92	330	330	9.1	2009.5	94
64	17	15	23.476	+1	19	23.59	16.3	0.49	390	390	4.3	2011.7	159
65	4	48	11.064	+48	32	20.63	17.4	0.88	390	7.9	6.3	2011.0	3102
66	16	35	13.811	+35	47	19.72	19.0	0.81	420	420	2.5	2011.2	244
67	4	18	25.230	+22	11	33.40	18.0	0.77	450	1.7	3.5	2006.4	2365
68	7	38	27.083	-27	28	0.96	17.6	0.99	460	0.8	2.5	2005.9	1743
69	12	38	41.040	-19	21	28.97	18.8	1.09	510	510	4.1	2011.6	26
70	20	33	59.516	+64	19	8.79	15.0	0.88	510	29	3.1	2006.8	978
71	18	32	54.168	+42	25	39.13	16.0	0.61	530	0.1	3.5	2014.2	2018
72	22	32	58.123	+53	47	44.03	17.3	0.88	550	27	15.7	2011.7	2409
73	16	8	14.289	-10	26	30.00	19.3	0.42	550	130	19.2	2013.2	6838
74	1	47	55.998	+60	7	28.79	16.8	0.38	580	89	1.5	2006.0	569
75	20	11	13.029	+16	11	11.76	16.8	0.53	590	180	5.4	2009.3	538
76	2	7	4.257	+49	38	37.02	17.9	0.03	600	600	7.2	2014.4	245
77	21	40	29.990	+54	0	33.34	16.3	0.61	630	200	4.6	2011.0	526
78	4	12	58.174	+52	36	35.12	16.2	0.61	630	55	7.0	2007.6	1018
79	17	42	10.234	-8	49	4.78	17.5	1.00	640	170	9.3	2009.6	591
80	7	11	12.027	+43	29	50.06	16.7	0.92	670	670	9.7	2014.2	241
81	1	48	49.863	+55	2	6.07	17.1	0.84	680	680	3.7	2013.2	90
82	19	38	32.540	-2	51	17.35	17.3	0.61	720	68	3.6	2012.2	705
83	13	8	25.653	+12	26	36.56	18.7	0.34	770	770	1.8	2006.3	45
84	18	8	7.264	-30	55	47.56	17.2	1.54	800	1.2	4.3	2012.9	1824
85	11	16	36.426	+53	5	3.39	18.6	0.45	890	0.9	2.6	2005.8	1980
86	12	33	49.377	+22	34	26.09	16.5	0.61	940	14	4.5	2010.8	3033
87	7	13	40.780	-13	28	15.00	18.5	0.38	1000	240	19.4	2014.2	6685
88	3	48	28.765	+51	14	10.45	19.1	0.53	1100	21	7.3	2013.3	3086
89	1	38	32.012	+47	32	16.07	16.3	0.26	1200	9.5	4.4	2009.6	2753
90	21	7	38.604	+66	20	48.27	17.6	0.65	1300	2.2	2.9	2013.8	1354
91	5	44	4.547	+40	56	36.53	18.0	0.53	1500	46	15.4	2012.4	2254
92	17	7	15.944	+19	25	42.32	18.0	0.53	1500	240	1.9	2010.4	496
93	12	21	50.168	+6	43	30.57	17.8	1.08	1800	750	5.3	2007.3	459
94	17	11	26.776	-14	47	54.85	17.3	0.57	2200	3.5	2.8	2005.2	2057
95	20	34	33.168	+7	57	34.35	15.5	0.81	2300	80	2.1	2005.0	1047
96	19	34	51.454	-12	21	12.16	17.6	0.42	2300	120	5.5	2008.5	3842
97	23	21	15.664	+1	2	23.84	18.5	0.49	2400	0.0	1.8	2005.6	957
98	23	21	15.664	+1	2	23.84	18.5	0.49	2400	0.0	1.8	2005.6	957
99	3	21	27.613	+46	57	35.37	19.3	0.42	2500	2.1	4.1	2012.9	1977
100	21	31	22.610	-5	11	19.26	15.5	0.65	2600	140	2.8	2007.0	920

Table 5—Continued

Event #	h	m	s	o	DEC ' "	V	B–V	τ hr	τ^* hr	d_{2000} "	t_0 yr	β mas
101	9	29	43.421	–17	32 55.89	18.5	0.49	2800	28	6.6	2014.3	1544
102	5	44	4.732	+40	56 36.92	16.2	0.61	2800	360	16.6	2013.0	4224
103	10	20	42.193	+20	27 45.69	13.6	0.61	3000	5.1	3.7	2010.9	2351
104	8	33	16.336	+40	56 1.54	17.4	0.92	3100	23	3.8	2011.4	2757
105	2	19	3.789	+35	21 14.03	19.2	0.22	3100	380	10.9	2013.7	863
106	19	36	8.131	–11	40 53.08	18.9	0.53	3400	2.7	2.6	2007.4	1884
107	12	38	32.897	+35	13 5.99	12.3	1.00	3700	0.0	4.3	2014.8	1646
108	21	10	58.630	+46	57 29.32	15.7	0.49	3800	230	3.1	2007.4	931
109	8	15	19.195	+4	55 34.93	16.1	0.42	4300	0.0	1.8	2008.2	289
110	13	14	8.423	+6	18 29.92	14.6	0.88	4300	0.0	3.2	2009.1	909
111	19	22	1.635	+7	2 24.64	15.7	1.04	4600	220	10.1	2011.4	3233
112	19	7	44.042	+32	32 48.04	17.7	0.30	4800	110	16.4	2010.0	2023
113	0	44	1.377	+75	12 24.32	16.9	0.69	5100	0.9	3.6	2010.1	1915
114	23	57	45.335	+23	18 4.96	16.9	0.96	5200	420	20.6	2014.0	2665
115	3	6	19.919	+51	3 20.01	15.9	0.73	5300	79	10.4	2012.0	2182
116	17	37	27.796	+71	3 52.42	18.8	0.73	6400	300	6.6	2013.5	1081
117	19	57	29.014	–17	30 19.75	17.1	0.67	6500	500	6.8	2013.5	931
118	18	47	14.940	–17	26 21.29	14.3	1.28	6700	52	4.5	2008.6	1701
119	5	48	24.169	+7	45 37.27	16.8	0.30	7300	300	2.3	2007.6	860
120	18	55	10.847	–9	3 31.87	18.7	0.49	7500	980	2.6	2007.7	681
121	5	49	57.019	+36	50 20.80	18.5	0.81	8100	170	3.5	2006.4	1393
122	15	29	29.887	–61	46 35.06	15.1	0.86	>10000	110	3.3	2008.4	2824
123	2	12	0.119	+32	21 43.17	17.1	0.53	>10000	550	5.7	2009.9	1126
124	0	1	46.608	+41	35 51.45	12.7	0.49	>10000	10	3.4	2008.9	2131
125	22	52	25.818	–22	20 10.75	18.3	0.83	>10000	300	4.2	2013.9	1000
126	18	41	10.805	+24	46 58.68	18.1	0.77	>10000	860	8.6	2015.0	4166
127	22	9	0.541	+70	41 52.30	17.5	0.73	>10000	8.0	2.8	2007.3	2144
128	8	52	31.013	+68	0 15.05	18.9	0.81	>10000	3.9	3.0	2011.8	2068
129	22	32	46.985	–5	57 17.76	18.1	0.18	>10000	270	2.4	2008.3	1014
130	10	17	10.789	+60	11 39.50	18.4	0.73	>10000	140	4.0	2009.8	2840
131	14	55	2.394	+43	1 29.81	13.3	0.77	>10000	150	3.9	2008.9	2879
132	15	27	45.232	–9	1 36.87	17.6	0.38	>10000	940	4.7	2014.6	848
133	3	0	59.817	+59	36 41.44	15.3	0.69	>10000	110	2.5	2009.9	1150
134	0	31	4.126	+36	40 35.67	15.5	0.77	>10000	310	2.7	2009.6	1002
135	18	15	13.582	–19	24 0.97	16.7	1.12	>10000	320	3.0	2007.0	1274
136	23	10	4.166	+63	57 52.23	18.6	0.92	>10000	250	5.3	2011.2	2858
137	23	9	37.757	+33	12 43.91	18.0	0.61	>10000	260	3.3	2008.3	1351
138	13	42	11.446	–5	59 11.55	18.0	0.14	>10000	3.8	3.9	2014.6	1959
139	23	15	25.660	+9	44 46.57	13.9	0.38	>10000	110	3.4	2005.7	2415
140	23	42	20.197	–13	56 22.20	14.7	0.96	>10000	0.0	2.8	2008.2	1397
141	21	52	12.127	+27	24 53.43	18.3	0.61	>10000	690	8.1	2009.9	1594
142	4	12	58.126	+52	36 37.43	17.7	1.00	>10000	780	5.5	2005.5	2343
143	21	36	11.207	+19	5 12.97	18.7	0.30	>10000	660	2.8	2007.8	1097
144	11	11	54.238	+3	37 28.13	19.0	0.81	>10000	110	5.3	2013.4	1775
145	23	49	23.226	–2	34 26.56	18.9	0.61	>10000	480	3.4	2012.4	1041
146	4	41	21.805	+22	54 21.73	17.9	0.81	>10000	380	4.7	2006.7	1835
147	17	30	22.591	+19	12 29.43	16.4	0.45	>10000	93	5.4	2012.8	2002
148	9	6	40.386	–30	12 24.63	18.7	1.15	>10000	14	2.3	2006.1	2008
149	17	18	47.074	–29	46 5.84	15.9	0.99	>10000	110	3.5	2010.5	2424
150	9	43	46.357	–7	3 54.17	19.5	0.30	>10000	500	6.3	2012.9	2722

Table 5—Continued

Event #	h	m	s	o	DEC '	''	V	$B-V$	τ hr	τ^* hr	d_{2000} ''	t_0 yr	β mas
151	15	24	37.078	−6	49	28.29	14.2	0.77	>10000	590	5.3	2009.6	2670
152	0	28	54.282	+50	22	36.54	18.2	0.45	>10000	180	4.4	2008.7	2155
153	23	47	53.845	−4	56	5.96	17.5	0.77	>10000	880	2.8	2013.1	956
154	17	46	23.180	−18	7	7.07	16.7	0.92	>10000	100	2.2	2007.6	1558
155	18	42	57.647	−11	8	57.84	18.2	1.20	>10000	150	4.6	2011.7	2049
156	0	9	53.777	+53	1	15.86	18.2	0.53	>10000	98	2.9	2009.5	1790
157	18	6	20.299	+2	3	3.83	16.9	0.81	>10000	220	4.9	2012.6	1947
158	7	30	8.140	+32	48	28.60	16.9	0.96	>10000	0.0	2.7	2011.5	899
159	20	31	56.874	−8	26	8.85	18.6	0.49	>10000	450	4.5	2014.5	2526
160	6	59	28.540	+19	30	33.29	17.7	0.73	>10000	260	3.6	2011.2	1696
161	14	4	48.734	−5	31	26.82	16.9	0.77	>10000	370	2.9	2006.2	2447
162	16	20	36.099	+29	15	0.77	13.6	0.53	>10000	200	4.8	2014.7	2221
163	19	31	30.054	+32	21	8.21	16.3	0.65	>10000	310	3.1	2008.0	1844
164	7	19	21.878	−19	4	43.75	16.8	0.80	>10000	98	2.6	2007.8	2154
165	17	0	42.201	−9	25	38.20	16.0	0.53	>10000	510	3.2	2008.6	1807
166	1	48	43.205	+38	16	13.22	18.6	0.81	>10000	510	3.7	2012.0	1691
167	5	57	28.542	+48	32	16.95	16.0	0.49	>10000	1000	4.7	2010.4	2314
168	18	55	10.936	−9	3	29.32	18.9	0.49	>10000	410	4.2	2011.0	2011
169	13	41	49.531	+47	0	8.19	15.2	1.00	>10000	0.0	2.9	2012.7	1434
170	2	8	44.489	+25	36	28.48	17.4	0.42	>10000	580	3.1	2006.7	2175
171	1	43	23.601	+62	39	23.65	16.6	0.61	>10000	420	2.0	2006.7	1525
172	7	20	2.327	+68	27	40.64	17.5	0.38	>10000	0.0	2.2	2007.9	1411
173	20	3	9.487	+61	2	49.74	18.5	0.57	>10000	570	2.2	2008.8	1521
174	21	13	8.386	−9	49	6.12	16.8	0.69	>10000	0.0	2.7	2013.3	1148
175	1	3	57.028	+79	40	21.50	16.7	0.81	>10000	600	2.8	2011.1	1606
176	16	50	22.517	−1	46	32.75	15.9	0.45	>10000	500	4.3	2014.6	2161
177	5	28	4.644	+54	55	30.78	17.7	0.69	>10000	860	2.6	2009.9	1554
178	21	0	36.351	−18	16	53.76	15.6	0.32	>10000	0.0	2.7	2010.7	1695
179	2	25	29.051	+44	47	38.70	18.4	0.49	>10000	370	2.4	2006.4	2034
180	18	7	41.398	+40	23	47.73	18.9	0.96	>10000	840	2.4	2008.7	1674
181	0	41	58.855	+57	48	3.20	18.9	0.49	>10000	500	2.9	2008.6	2092

Numeration follows the lens number in tables 4. Source star’s right ascension and declination are at plate epoch, equinox J2000. Visual magnitude is in Tycho, and color in Johnson system (see § 3.1). Event is described by τ (*SIM* observing time), τ^* (*SIM* observing time with reduced impact parameter), d_{2000} lens-source separation in year 2000.0, t_0 time of closest approach and β , the minimum impact parameter.